Dynamics of a dilute sheared inelastic fluid. I. Hydrodynamic modes and velocity correlation functions

V. Kumaran
Department of Chemical Engineering, Indian Institute of Science, Bangalore 560 012, India
(Received 2 July 2008; published 14 January 2009)

The hydrodynamic modes and the velocity autocorrelation functions for a dilute sheared inelastic fluid are analyzed using an expansion in the parameter $\epsilon=(1-e)^{1/2}$, where e is the coefficient of restitution. It is shown that the hydrodynamic modes for a sheared inelastic fluid are very different from those for an elastic fluid in the long-wave limit, since energy is not a conserved variable when the wavelength of perturbations is larger than the "conduction length." In an inelastic fluid under shear, there are three coupled modes, the mass and the momenta in the plane of shear, which have a decay rate proportional to $k^{2/3}$ in the limit $k\to 0$, if the wave vector has a component along the flow direction. When the wave vector is aligned along the gradient-vorticity plane, we find that the scaling of the growth rate is similar to that for an elastic fluid. The Fourier transforms of the velocity autocorrelation functions are calculated for a steady shear flow correct to leading order in an expansion in ϵ. The time dependence of the autocorrelation function in the long-time limit is obtained by estimating the integral of the Fourier transform over wave number space. It is found that the autocorrelation functions for the velocity in the flow and gradient directions decay proportional to $t^{-5/2}$ in two dimensions and $t^{-15/4}$ in three dimensions. In the vorticity direction, the decay of the autocorrelation function is proportional to t^{-3} in two dimensions and $t^{-7/2}$ in three dimensions.

DOI: 10.1103/PhysRevE.79.011301 PACS number(s): 45.70.−n, 45.50.−j, 51.10.+y

I. INTRODUCTION

Flowing granular matter falls into an interesting class of nonequilibrium phenomena involving dissipative processes, where the laws of thermodynamics cannot be easily adapted. The molecules in a molecular fluid are "fluidized" by thermal fluctuations, and this facilitates rearrangement of molecules and flow in response to external stresses. The density of states of the equilibrium fluid is given by the Boltzmann distribution. This also provides access to dynamical properties for a fluid near equilibrium, since the stress response can be related to the correlations in the fluctuating fields at equilibrium via the fluctuation-dissipation relations [1]. In a granular material with grains of macroscopic size, the thermal fluctuations are vanishingly small and the fluidization of particles requires external forcing, either in the form of mean shear or in the form of forcing at the boundaries. Consequently, there is no "equilibrium" at which we have a prescribed distribution of states. In the absence of a known equilibrium distribution, it is also not possible to formulate fluctuation-dissipation relations for dynamical properties.

An alternative approach, applied in the kinetic theory of gases, is to use the Boltzmann equation to calculate both equilibrium distribution and the dynamical properties near equilibrium. This approach involves an important assumption, the molecular chaos assumption, which states that the two-particle distribution function is the product of the single-particle distribution functions. Using this assumption, the Boltzmann equation shows that the velocity distribution function is a Maxwell-Boltzmann distribution. In effect, the distribution of states is obtained as a result from the molecular chaos and is not an assumption of equilibrium thermodynamics. Dynamical properties near equilibrium can be evaluated quite easily by imposing an external stress or heat flux and evaluating the resulting corrections to the distribution function. However, because of the molecular chaos assumption, this approach can be used only for very dilute gases where binary collisions dominate and where molecules move distances long compared to their diameter between successive collisions, so that the pre collisional velocities of a pair of colliding molecules are uncorrelated.

Kinetic theories for granular materials [2–8] make use of the analogy between the motion of molecules in a dilute gas and the motion of particles in a granular flow, while recognizing the important distinction that the collisions between particles are inelastic and energy dissipating. The energy dissipation in collisions enters through the coefficient of restitution, e, which is the ratio of the magnitudes of the post- and pre-collisional relative velocities along the line joining the centers of the particles. For perfectly elastic collisions ($e=1$), energy is conserved and the distribution function is a Maxwell-Boltzmann distribution. For inelastic collisions, an asymptotic expansion is used in powers of $\epsilon=(1-e)^{1/2}$, where the leading-order distribution function is the Maxwell-Boltzmann distribution. However, the temperature in this distribution is not determined from thermodynamic considerations, but rather by a balance between the rate of supply of energy (due to shear or forcing at the boundaries) and the rate of dissipation of energy. Constitutive models have been developed for granular flows using methods similar to those used in the kinetic theory of gases, and these result in conservation equations similar to the Navier-Stokes equations, with the important difference that there is a dissipation term in the energy balance equation. An important assumption made in these kinetic theory calculations is the molecular chaos approximation, which neglects the effect of correlated collisions between particles. Due to this, these theories are generally assumed to be valid only in the dilute limit.

The stability analysis of an unbounded linear shear flow is different from that for bounded parallel flows, because if the

mean velocity profile is linear, the velocity profile tends to infinity as the coordinate in the gradient direction goes to infinity. Due to this, it is not possible to obtain a dispersion matrix with constant coefficients for an unbounded linear shear flow in which the perturbations are in the form of Fourier modes. A dispersion matrix with constant coefficients can only be obtained for the special case where the component of the wave vector in the flow direction is zero. For more general perturbations which are modulated in the flow direction, the dispersion matrix contains a derivative with respect to the component of the wave vector in the gradient direction, and it is necessary to solve an ordinary differential equation in wave vector space, as was done by Ernst *et al.* [9]. It is possible to effect a transform where the wave vector is a function of time and which rotates with the mean shear [10]. With this transformation, the derivative with respect to the wave vector is no longer present in the dispersion matrix, but now the wave vector in the dispersion matrix is a function of time. Therefore, in contrast to the linear stability analysis, the perturbations are not exponentially growing or decaying in time. It is also difficult to obtain analytical solutions for the growth rates and the eigenfunctions of the dispersion matrix, as discussed in the present work.

This difficulty was realized early on in the stability analysis of sheared granular flows by Savage [11] and Babic [12], who analyzed continuum mass, momentum, and energy equations. These authors realized that the dispersion relation was a function of time and restricted attention to the evaluation of the growth rates at the initial time ($t=0$) when the perturbation is applied. While they reached the conclusion that the initial growth rates are positive (perturbations are unstable) for a wide range of wave numbers, these studies are also careful to acknowledge that the development of disturbances at later times could be affected by the turning of the wave vector. The numerical calculations of Alam and Nott [13] showed that the turning of the wave vector has a stabilizing effect for perturbations with a nonzero wave vector component in the flow direction. Though the linear stability analysis predicts a growth of perturbations at the initial time, this transient growth is followed by a decay as the wave vector turns and gets aligned with the gradient direction in the long-time limit. Therefore, for unbounded linear shear flows with a nonzero component of the wave vector along the flow direction, there is initial transient growth of perturbations. However, these decay in the long-time limit due to the turning of the wave vector by the mean shear, thus rendering the system stable in the long-time limit. It should be noted that transient growth does not imply a change of base state. The linear analysis does predict whether the system is stable or unstable, but it does not predict what other state the system goes to in case it is unstable. It is necessary to do the nonlinear calculation to determine the change in base state. This is not done in the present case, because the linear analysis has predicted that the system is stable in the long-time limit.

While the above results were mostly obtained using numerical calculations designed to identify domains in parameter space where the flow is unstable, an asymptotic analysis was carried out by the author [14] in the long-wave limit. This was based on the rationale that the hydrodynamic equations are valid only when the length scale is large compared to the microscopic scale (particle diameter or mean free path), and this provides the following physical insights into the hydrodynamic modes of sheared inelastic fluids. In addition to the microscopic scale, there is another length scale of relevance for a nearly elastic fluid, which is the conduction length $\lambda/(1-e)^{1/2}$, where λ is the microscopic scale and e is the coefficient of restitution. This length scale arises from a balance between the rates of conduction and dissipation of energy in the energy balance equation, as discussed a little later on. For length scales small compared to the conduction length, the rate of conduction of energy is large compared to the rate of dissipation and energy can be considered a conserved variable. If the rate of dissipation (and production) is neglected in the leading approximation, then we recover the $D+2$ hydrodynamic modes (mass and D components of momentum and energy) for an elastic fluid, where D is the dimensionality of the system. When the length scale is large compared to the conduction length, the rate of conduction of energy is small compared to the rate of dissipation. Energy is a nonconserved variable in this case, and there are only $D+1$ hydrodynamic modes (mass and D components of the momentum) whose growth rates decrease to zero in the long-wave limit. Of, these, it was found that there are three modes whose growth rate scales as $k^{2/3}$ in the long-wave limit $k\rightarrow 0$, where k is the wave number. This is very different from the growth rates of the hydrodynamic modes in an elastic fluid, for which the two propagating modes have a decay rate with imaginary part proportional to k and real part proportional to k^2, while D diffusive modes ($D-1$ transverse momenta and one energy mode) have real decay rate proportional to k^2 in the limit $k\rightarrow 0$. The transition from $k \gg \lambda/(1-e)^{1/2}$ (where energy is a slow conserved variable) to $k \ll \lambda/(1-e)^{1/2}$ (where energy is a nonconserved fast variable) was analyzed numerically, and the scaling laws in the two regimes were verified.

The small-wave-number analysis discussed above was also carried out using a time-dependent wave vector which rotates with the mean shear and aligns with the gradient direction in the long-time limit. In the limit $k \ll \lambda/(1-e)^{1/2}$, perturbations were found to have positive growth rates in the short-time limit. However, the initial growth of perturbations is followed by a decay in the long-time limit due to the turning of the wave vector [14]. An identical conclusion was obtained by Alam and Nott [13] for granular flows in the dilute limit in the absence of friction. In our linear stability analysis here, we obtain the same result.

For the special case where the wave vector is aligned in the gradient direction (layering modes), there is no rotation of the wave vector. The perturbations are found to be stable for an unbounded linear shear flow in the limit of small volume fraction, both in the numerical calculations of Alam and Nott [13] and in analytical calculations in the long-wave limit [14]. This is different from the result of Lee and Dufty [15], who found the uniform shear flow to be unstable to layering modes in the long-wave limit; the scaling of the growth rate is also different from that obtained using the small-wave-number asymptotic analysis by the author [14]. We have examined the reasons for this, and we find that this is due to a difference in the formulation of the hydrodynamic

matrix in the two cases. Lee and Dufty [15] consider a linear shear flow in which an external thermostat is used to enforce the constant temperature condition. Due to this, the part of their hydrodynamic matrix which is independent of k [Lee and Dufty [15], Eq. (4.8)] does not contain contributions from the energy balance equation. In the present analysis, we incorporate the energy dissipation due to inelastic collisions, and therefore there is a nonzero contribution to the hydrodynamic matrix in the limit $k \to 0$ due to the terms in the energy balance equation [Eq. (31) below]. Using the formulation presented here, we find that the layering modes are stable; this is consistent with the conclusions of Alam and Nott [13] for the frictionless case, as also with thus earlier studies of Savage [11] and Babic [12]. Thus we can conclude that the uniform shear flow of inelastic fluid is a well-defined stable steady state.

There are instabilities in bounded channel flows, however, due to the wall boundary conditions [16,17]. This is due to the boundary conditions imposed at the walls, and this could lead to layering either at the walls or at the center, depending on the boundary conditions. All of these linear stability studies assume that the constitutive relations obtained from kinetic theory are applicable to real granular flows and that correlation effects are not important. In elastic fluids, it is well known that correlations do result in a diverging viscosity in two dimensions and diverging Burnett coefficients in three dimensions, as discussed below. If such divergences carry over unaltered to sheared inelastic fluids, then the continuum approximations used in the above stability studies are not valid. Therefore, it is important to examine the effect of correlations to determine whether they result in a significant modification of the constitutive relations.

It is well known that correlated collisions cause a significant change in the form of the constitutive relations for fluids at equilibrium. The seminal studies of Kawasaki and Gunton [18] and Yamada and Kawasaki [19] using mode-coupling theory, Ernst and Dorfman [20] and Ernst *et al.* [9] using the ring-kinetic theory, and Lutsko and Dufty [10] using a generalized Langevin formulation showed that the shear viscosity in a fluid of elastic particles is a nonanalytic function of the strain rate. In two dimensions, the shear viscosity has the form $\eta = \eta_0 + \eta' \ln(\dot{\gamma})$, while in three dimensions the shear viscosity has the form $\eta = \eta_0 + \eta' |\dot{\gamma}|^{1/2}$, where η_0 is the shear viscosity for a Newtonian fluid and $\dot{\gamma}$ is the strain rate. This implies that the coefficient of viscosity diverges in a two-dimensional fluid, while the Burnett coefficients diverge in a three-dimensional fluid. It is well known that the viscosity renormalization is caused by the long-time tails in the velocity autocorrelation functions [9,21], where the autocorrelation functions decay as a power law $t^{-D/2}$ in the long-time limit, where D is the dimension of the system [22–26].

It is important to note that the calculation of Ernst and Dorfman [20] and Ernst *et al.* [9] were carried out for the sheared state of the fluid and the terms up to $O(\dot{\gamma})$ were included in the expansion in the limit $\dot{\gamma} \to 0$. When a fluid is sheared, there is viscous heating, due to which there is a continuous rise in temperature. This viscous heating, proportional to the product of the stress and strain rate, was not included because it is $O(\dot{\gamma}^2)$. The lack of a steady state when the $O(\dot{\gamma}^2)$ term is included implies that the next-higher-order terms in the series may not exist for a steady shear flow. Heating is prevented by imposing a thermostat on the system of elastic particles or by energy dissipation due to the dissipation by inelastic collisions. In either case, heating can be prevented only if there is energy dissipation in the system. This dissipation makes a difference in the energy conservation equation in the long wavelength limit and changes the nature of the hydrodynamic modes. This because the rate of dissipation of energy in the energy conservation equation is proportional to $D_T k^2$, where D_T is the thermal diffusivity and k is the wave number, whereas the rate of dissipation is independent of k for $k \to 0$. Therefore, there is a range of wave numbers for which the rate of dissipation of energy is large compared to the rate of conduction and energy has to be considered a nonconserved mode for this range of wave numbers.

The distinction between the conserved and nonconserved nature of energy can be explained in another manner [14,27–32]. The rate of conduction of energy per unit volume is proportional to $\rho D_T T / L^2$, where L is a characteristic length and D_T, the thermal diffusivity, is proportional to $T^{1/2}\lambda$, where ρ is the number density and λ is the mean free path (the mass of a particle is assumed to be 1 without loss of generality). The rate of dissipation of energy is proportional to $(1-e)\rho T^{3/2}/\lambda$, since the energy dissipation in a collision is proportional to $(1-e)T$, and the frequency of collisions is proportional to $T^{1/2}/\lambda$. If we compare the rates of conduction and dissipation, a balance between these is achieved only if the length scale $L \ll \lambda/\epsilon$, or $k \gg \epsilon/\lambda$, where $\epsilon = (1-e)^{1/2}$ is a small parameter which quantifies the departure from elastic collisions. For wave numbers $k \gg \epsilon/\lambda$, the rate of conduction is large compared to the rate of dissipation and energy can be treated as a conserved field. For wave numbers $k \ll \epsilon/\lambda$, the rate of conduction of energy is small compared to the rate of dissipation and it is necessary to treat energy as a nonconserved variable. As expected, the conduction length is infinity for a perfectly elastic system, since the energy is conserved throughout the domain in this case.

The hydrodynamic modes for $k \ll \epsilon/\lambda$ are very different from those for an elastic fluid. In an elastic fluid, the growth rates of the conserved modes are as follows. There are two propagating modes, whose growth rates have an imaginary part proportional to the wave number k and a real negative part proportional to k^2 in the limit $k \to 0$. There are two transverse shear modes and one energy diffusion mode, all of which have decay rates proportional to k^2. In an inelastic fluid for $k \ll \epsilon/\lambda$, we find that there are three modes, corresponding to mass and momentum fluctuations in the plane of shear, which have decay rates proportional to $k^{2/3}$. There is one transverse momentum mode with decay rate proportional to k^2, while energy perturbations have a finite decay rate in the limit $k \to 0$. Thus, the decay of the linear hydrodynamic modes in a sheared inelastic fluid is very different from that in an elastic fluid. Recent work has suggested that the decay of the velocity autocorrelation function in sheared granular flows could be faster. For sheared dense granular flow, Ostuki and Hayakawa [33] used mode-coupling theory to obtain the decay proportional to $t^{-(D+2)/2}$, where D is the system dimension. The analysis of Kumaran [31] was based on incorporating correlations using the ring-kinetic equation for a

dense gas. This analysis suggested a faster decay in the velocity autocorrelation function proportional to $t^{-3D/2}$, though the form of the autocorrelation function was not explicitly calculated. Here, we examine the exact form of the autocorrelation function from the decay rates of the hydrodynamic modes in the limit where energy is treated as a nonconserved variable.

It is important to note the following features of the hydrodynamic modes of the Boltzmann or Navier-Stokes equations for a sheared inelastic fluid [14]. Since the system is under a linear shear flow, it is not possible to obtain an eigenvalue problem if the wave vector is time independent. It is necessary to define a wave vector that rotates with the flow and is a linear function of time in order to obtain an eigenvalue problem. Since the wave vector is dependent on time, the growth rates that are calculated are also time dependent. An asymptotic expansion in wave number can be used to calculate the growth rates, and the resulting expressions contain contributions proportional to $k^{2/3}$, $k^{4/3}$, and k^2. The terms proportional to $k^{2/3}$ dominate in a small-k expansion only at short times, and some of the modes have growth rates with positive real parts, indicating that perturbations are unstable in the short-time limit. However, since the wave number is increasing with time, at long times the k^2 terms become dominant and exerts a damping effect on the perturbations. This implies that hydrodynamic fluctuations are unstable at short times, but are stable in the long-time limit. This enables us to define a stable steady state as the base state for the calculations. The calculation of the hydrodynamic modes, which are the eigenfunctions of the linear hydrodynamic equations, are complicated by the time dependence of the eigenvalues. It is not possible to use simple exponential relaxations, and a more complicated iterative procedure has to be used. This is outlined in the present calculation. Based on the decay rates of the hydrodynamic modes, we estimate the time decay of the velocity autocorrelation functions in the long-time limit. These results are used in Part II to study the effect of correlations on the dynamics of a dilute sheared inelastic fluid.

II. ANALYSIS

The system consists of smooth, inelastic particles (disks or spheres) of diameter d subject to a mean flow, in which the rate of deformation tensor is given by $\partial u_i/\partial x_j = G_{ij}$. The mass of the particles is set equal to 1, so that mass dimension in all dynamical variables is scaled by the particle mass. The collision rules used here are those for smooth inelastic particles, where the post-collisional relative velocity along the line joining centers is $-e$ times the precollisional relative velocity, while the post-collisional relative velocity perpendicular to the line joining centers is unchanged. Here, e is the normal coefficient of restitution. We consider a coordinate system where the mean velocity is along the x direction, the gradient is along the y direction, and the z direction is along the vorticity axis perpendicular to the plane of flow. At steady state, there is a balance between the rate of production of energy due to mean shear, μG_{xy}^2, and the rate of dissipation of energy due to inelastic collisions. The rate of dissipation of energy is proportional to $\rho T^{3/2}(1-e^2)/\lambda$, since the dissipation of energy in a collision is proportional to $(1-e^2)T$ and the collision frequency is proportional to $T^{1/2}/\lambda$, where $T^{1/2}$ is the magnitude of the fluctuating velocity, $\lambda \sim 1/\rho d^{D-1}$ is the mean free path, ρ is the number density, the mass of a particle is assumed to be 1, and D is the dimensionality of the system. We consider the near elastic limit $e \to 1$, where $\epsilon = (1-e)^{1/2}$ is a small parameter. In this case, it is easy to see that the strain rate is related to the temperature by $G_{xy} \sim \epsilon(T^{1/2}/\lambda)$. Since we scale all velocities in the analysis by $\bar{T}^{1/2}$ and all lengths by $1/\bar{\rho}d^{D-1}$, where $\bar{T}$ and $\bar{\rho}$ are the mean temperature and number density, respectively, we set $G_{xy} = \epsilon\dot{\gamma}$, where $\dot{\gamma}$ is $O(1)$ in the limit $\epsilon \to 0$.

We next turn to the Boltzmann equation for the single-particle distribution. In order to simplify the notation, Greek subscripts α, β, ξ are used for particle labels and capital Roman subscripts I, J, K are used to denote components of matrices a little later, so that they are not confused with the small Roman superscripts in the indicial notation for vectors. It is also useful to note at this stage that the number of subscripts in the joint distribution function f indicates the order of the distribution; for example, f_α is the single-particle distribution function for finding a particle at $(\mathbf{x}_\alpha, \mathbf{u}_\alpha)$, $f_{\alpha\beta}$ is the two-particle distribution function, which gives the simultaneous probability of finding two particles at the locations $(\mathbf{x}_\alpha, \mathbf{u}_\alpha)$ and $(\mathbf{x}_\beta, \mathbf{u}_\beta)$, and so on.

It is convenient to express the particle velocity as the sum of the mean velocity $\mathbf{U}$ which is a function of position and the fluctuating velocity $\mathbf{c}_\alpha = \mathbf{u}_\alpha - \mathbf{U}(\mathbf{x}_\alpha)$. The distribution function f_α then becomes a function of $(\mathbf{x}_\alpha, \mathbf{c}_\alpha, t)$, and the equation for the single-particle distribution is given by [34]

$$\frac{Df_\alpha}{Dt} + \frac{\partial(\mathbf{c}_\alpha f_\alpha)}{\partial \mathbf{x}_\alpha} - \mathbf{G}:\mathbf{c}_\alpha \frac{\partial f_\alpha}{\partial \mathbf{c}_\alpha} = \int_\beta C_{\alpha\beta}[f_{\alpha\beta}], \tag{1}$$

where the substantial derivative $D/Dt \equiv \partial/\partial t + \mathbf{U}\cdot\boldsymbol{\nabla}$, and $\mathbf{G} = (\partial \mathbf{U}/\partial \mathbf{x})$ is the rate of deformation tensor. In the above equation, the first term on the left is the rate of change of the distribution function in a reference frame moving with the local mean velocity, while the second term on the left is the rate of change of the distribution function due to the acceleration acting on the particle minus that due to the acceleration of the mean flow. The third term on the left accounts for the variation in distribution function due to particle translation, wherein the fluctuating velocity of the particle changes when a particle translates from one position to another because the mean velocity at the two locations is different even though the absolute velocity of the particle has not changed. The form of the collision integral on the right-hand side of Eq. (1) is

$$C_{\alpha\beta}(f_{\alpha\beta}) = \int_{\mathbf{n}} [e^{-2} f_{\alpha\beta}(\mathbf{c}'_\alpha, \mathbf{c}'_\beta, -\mathbf{x}_{\alpha\beta}) - f_{\alpha\beta}(\mathbf{c}_\alpha, \mathbf{c}_\beta, \mathbf{x}_{\alpha\beta})](\mathbf{u}_\alpha - \mathbf{u}_\beta)\cdot\mathbf{n} d^{D-1}, \tag{2}$$

where $\mathbf{n}$ is the unit vector along the line joining the centers of the particles at contact, directed from particle α to particle β, and d is the particle diameter. The integral $\int_{\mathbf{n}}$ is an integral over all possible orientations of $\mathbf{n}$, chosen in such a

manner that $(\mathbf{u}_\alpha - \mathbf{u}_\beta)\cdot\mathbf{n} > 0$ for colliding particles. The velocities $\mathbf{c}'_\alpha$ and $\mathbf{c}'_\beta$ are the velocities of the particles for the inverse "restituting" collision, which results in a gain of particles with velocities $\mathbf{c}_\alpha$ and $\mathbf{c}_\beta$, and the velocities $\mathbf{c}'_\alpha$ and $\mathbf{c}'_\beta$ are determined, for a given value of $\mathbf{n}$, using the collision rules. The factor $1/e^2$ incorporates the Jacobian for the transformation from $(\mathbf{c}'_\alpha, \mathbf{c}'_\beta)$ to $(\mathbf{c}_\alpha, \mathbf{c}_\beta)$, as well as the ratio of the relative normal velocities of the restituting and direct collisions. The collision integral can be separated into two parts: the first is the collision integral for elastic collisions, and the second is the correction to the collision integral due to the inelasticity of the particles:

$$C_{\alpha\beta}(f_{\alpha\beta}) = C^E_{\alpha\beta}(f_{\alpha\beta}) + C^I_{\alpha\beta}(f_{\alpha\beta}), \tag{3}$$

where the elastic part of the collision integral is

$$C^E_{\alpha\beta}(f_{\alpha\beta}) = \int_{\mathbf{n}} [f_{\alpha\beta}(\mathbf{c}''_\alpha, \mathbf{c}''_\beta, -\mathbf{x}_{\alpha\beta}) - f_{\alpha\beta}(\mathbf{c}_\alpha, \mathbf{c}_\beta, \mathbf{x}_{\alpha\beta})](\mathbf{u}_\alpha - \mathbf{u}_\beta)\cdot\mathbf{n}\, d^{D-1}, \tag{4}$$

where $\mathbf{c}''_\alpha$ and $\mathbf{c}''_\beta$ are the velocities of the elastic inverse "restituting" collision, which are determined, for a given value of $\mathbf{n}$, using the collision rules with $e=1$. The inelastic part of the collision integral is

$$C^I_{\alpha\beta}(f_{\alpha\beta}) = \int_{\mathbf{n}} [(1/e^2) f_{\alpha\beta}(\mathbf{c}'_\alpha, \mathbf{c}'_\beta, -\mathbf{x}_{\alpha\beta}) - f_{\alpha\beta}(\mathbf{c}''_\alpha, \mathbf{c}''_\beta, -\mathbf{x}_{\alpha\beta})] \times (\mathbf{u}_\alpha - \mathbf{u}_\beta)\cdot\mathbf{n}. \tag{5}$$

While the elastic part of the collision operator is inherently nonlocal in the velocity co-ordinates, the inelastic part can be expressed in a gradient expansion, since the differences $|\mathbf{c}'_\alpha - \mathbf{c}''_\alpha| \sim \epsilon^2 |\mathbf{c}''_\alpha|$ and $|\mathbf{c}'_\beta - \mathbf{c}''_\beta| \sim \epsilon^2 |\mathbf{c}''_\beta|$. Therefore, $C^I_{\alpha\beta}$ is $O(\epsilon^2)$ smaller than $C^E_{\alpha\beta}$.

In the present analysis, we use the molecular chaos approximation to write $f_{\alpha\beta}(\mathbf{x}_\alpha, \mathbf{x}_\beta, \mathbf{c}_\alpha, \mathbf{c}_\beta, t) = f_\alpha(\mathbf{x}_\alpha, \mathbf{c}_\alpha, t) \times f_\beta(\mathbf{x}_\beta, \mathbf{c}_\beta, t)$. This assumption is relaxed in Part II, where we consider the effects of correlations. The steady solution for the Boltzmann equation is obtained using an expansion in the small parameter ϵ. In the leading approximation, the collision integral is set equal to zero and the solution for the distribution function is the Maxwell-Boltzmann distribution

$$F_\alpha(\mathbf{c}_\alpha) = \frac{1}{(2\pi \bar{T}^{D/2})} \exp\left(-\frac{c_\alpha^2}{2\bar{T}}\right), \tag{6}$$

where $\bar{T}$ is the mean temperature. The steady distribution is expanded in a series in the small parameter ϵ as

$$f^s_\alpha(\mathbf{c}_\alpha) = F_\alpha(\mathbf{c}_\alpha)[1 + h_\alpha(\mathbf{c}_\alpha)]. \tag{7}$$

We define the stress tensor as $\mathbf{G} = \epsilon\dot{\gamma}\mathbf{e}_x\mathbf{e}_y$, and the first correction to the Boltzmann equation becomes

$$-\epsilon\dot{\gamma} c_x \frac{\partial F}{\partial c_y} = \int_\beta F_\alpha F_\beta C_{\alpha\beta}[h_\alpha + h_\beta]. \tag{8}$$

Note that the effect of the inelasticity in the collision operator appears only in the $O(\epsilon^2)$ correction to the Boltzmann equation.

The hydrodynamic modes are obtained by perturbing the distribution function:

$$f_\alpha(\mathbf{c}_\alpha) = f^s_\alpha(\mathbf{c}_\alpha)[1 + f'_\alpha(\mathbf{c}_\alpha)], \tag{9}$$

where $f'(\mathbf{c})$ is a small perturbation. The contributions to $f'(\mathbf{c}_\alpha)$ can be separated into two parts, the first of which are the "conserved variables" which are collisional invariants (the sum of the conserved variables of the two particles remains unchanged in a collision) and the "nonconserved variables." Since the conserved variables are unchanged in a collision, perturbations to the macroscopic fields corresponding to these variables do not decay in the long-wave limit and the decay rates of these perturbations goes to zero for $k \to 0$. In contrast, the macroscopic fields corresponding to the nonconserved variables decay over times scales comparable to the inverse of the collision frequency. There are five conserved modes in three dimensions for a system with elastic interparticle collisions: the mass, the three components of the momentum, and the energy. The Navier-Stokes equations are obtained by multiplying the Boltzmann equation by the particle mass, momentum, and energy and integrating over the velocities of the particles. For definiteness, we define the vector of conserved variables as

$$\Phi = (1, (c_{\alpha x}/\sqrt{\bar{T}}), (c_{\alpha y}/\sqrt{\bar{T}}), (c_{\alpha z}/\sqrt{\bar{T}}), \sqrt{D/2}[(c_\alpha^2/\bar{T}D) - 1]), \tag{10}$$

where D is the dimensionality. Equation (10) is applicable for three dimensions; the vector of conserved variables for two dimensions is obtained by removing the fourth element $(c_{\alpha z}/\sqrt{\bar{T}})$. Note that the basis vector is defined to be orthonormal, so

$$\int_\alpha F_\alpha \phi_{\alpha I} \phi_{\alpha J} = \delta_{IJ}. \tag{11}$$

Here and in the following analysis, capital subscripts such as $I, J, \ldots$ denote elements of a matrix and repeated subscripts imply a summation.

The dispersion relations for the conserved modes can be evaluated in two ways. One is from the linearized Boltzmann equation, which involves inserting Eq. (9) into the Boltzmann equation (1) and linearizing in the perturbation f'_α. The resultant equation is multiplied by the conserved modes and integrated over velocity space to obtain the dispersion relations. The second is to use the Navier-Stokes equations, which are obtained by multiplying the Boltzmann equation by mass, momentum, and energy and integrating over the particle velocity. Both of these give identical results for the dispersion relations. Here, we use the linearized Navier—Stokes equations to evaluate the growth rate of the hydrodynamic modes, since the physical interpretation is easier. The Navier-Stokes equations are

$$\frac{\partial \rho}{\partial t} + \nabla\cdot(\rho\mathbf{u}) = \mathbf{0}, \tag{12}$$

$$\rho\left(\frac{\partial \mathbf{u}}{\partial t} + \mathbf{u}\cdot\nabla\mathbf{u}\right) = -\nabla p + \nabla\cdot\tau, \tag{13}$$

$$\rho C_v\left(\frac{\partial T}{\partial t}+\mathbf{u}\cdot\boldsymbol{\nabla}T\right)=\boldsymbol{\nabla}\cdot(K\,\boldsymbol{\nabla}\,T)-p(\boldsymbol{\nabla}\cdot\mathbf{u})+\tau.(\boldsymbol{\nabla}\mathbf{u})-D, \tag{14}$$

where ρ, $\mathbf{u}$, and T are the density, mean velocity, and temperature fields, p is the pressure which is related to the density and temperature through an equation of state, K is the thermal conductivity, and the specific heat $C_v=(D/2)$, where D is the spatial dimension. The stress tensor τ is

$$\tau=\mu[\boldsymbol{\nabla}\mathbf{u}+(\boldsymbol{\nabla}\mathbf{u})^{+}]+[\mu_b-(2\mu/3)]\mathbf{I}(\boldsymbol{\nabla}\cdot\mathbf{u}), \tag{15}$$

where μ and μ_b are the shear and bulk viscosities, and the superscript $+$ denotes the transpose. The last term on the right-hand side of the energy equation (14) is the rate of dissipation of energy due to inelastic collisions, which is not present for an elastic fluid. In the linear analysis, small perturbations are imposed on the density, mean velocity, and temperature fields,

$$\rho=\bar{\rho}(1+\rho'),$$

$$u_x=\bar{T}^{1/2}(\epsilon\dot{\gamma}y+u_x'),$$

$$u_y=\bar{T}^{1/2}u_y',$$

$$u_z=\bar{T}^{1/2}u_z',$$

$$T=\bar{T}(1+T'), \tag{16}$$

and the equations are linearized in the perturbations denoted by the primes. The perturbations to the density, velocity, and temperature fields also result in perturbations to the pressure, viscosity, conductivity, and the rate of dissipation of energy. The expressions for these can be simplified by realizing that for a gas of hard particles, there is no intrinsic energy scale for interparticle interactions. Consequently, the pressure has to be proportional to the temperature, the viscosity and thermal diffusivity are proportional to the square root of temperature, and the rate of dissipation or energy is proportional to the 3/2 power of the temperature. Therefore, these can be expressed as

$$p=\bar{\rho}\bar{T}(\bar{p}^{\dagger}+p_{\rho}^{\dagger}\rho'+\bar{p}^{\dagger}T'),$$

$$\mu=(\bar{T}^{1/2}/d^{D-1})[\bar{\mu}^{\dagger}+\bar{\mu}_{\rho}^{\dagger}\rho'+(\bar{\mu}^{\dagger}/2)T'],$$

$$\mu_b=(\bar{T}^{1/2}/d^{D-1})[\bar{\mu}_b^{\dagger}+\bar{\mu}_{\rho}^{\dagger}\rho'+(\bar{\mu}^{\dagger}/2)T'],$$

$$K=(\bar{T}^{1/2}/d^{D-1})[\bar{K}^{\dagger}+\bar{K}_{\rho}^{\dagger}\rho'+(\bar{K}^{\dagger}/2)T'],$$

$$D=(\bar{\rho}^2d^{D-1}\epsilon^2\bar{T}^{3/2})[\bar{D}^{\dagger}+\bar{D}_{\rho}^{\dagger}\rho'+(3\bar{D}^{\dagger}/2)T'], \tag{17}$$

where the overbar denotes the value of the variable in the base flow and $\star_{\rho}\equiv\bar{\rho}\,(\partial\star/\partial\rho)|_{\rho=\bar{\rho}}$.

Some general comments can be made about the nature of the coefficients in Eq. (17), which is independent of whether the system is two dimensional or three dimensional. For an dilute gas of spherical monoatomic particles in both two and three dimensions, the coefficients for the pressure assume equal values, $\bar{p}^{\dagger}=1$ and $\bar{p}_{\rho}^{\dagger}=1$. In addition, the bulk viscosity is zero, $\bar{\mu}_b^{\dagger}=0$, and the shear viscosity and thermal conductivity are independent of volume fraction, $\bar{\mu}_{\rho}^{\dagger}=\bar{K}_{\rho}^{\dagger}=0$. From energy balance at steady state, we find that $\bar{D}^{\dagger}=\bar{\mu}^{\dagger}\dot{\gamma}^2$. In addition, since the dissipation is due to inelastic collisions, the derivative of the dissipation rate with density is given by $\bar{D}_{\rho}^{\dagger}=2\bar{D}^{\dagger}$. The values of coefficients in the dynamical coefficients obtained by truncating the Sonine polynomial expansion at the first term differ in two and three dimensions. In three dimensions, the values of the coefficients are $\bar{\mu}^{\dagger}=(5/16\sqrt{\pi})$, $\bar{\mu}_{\rho}^{\dagger}=0$, $\bar{\mu}_b^{\dagger}=0$, $\bar{\mu}_{b\rho}^{\dagger}=0$, $\bar{K}^{\dagger}=(75/64\sqrt{\pi})$, $\bar{K}_{\rho}^{\dagger}=0$, $\bar{D}^{\dagger}=4\sqrt{\pi}$, and $\bar{D}_{\rho}^{\dagger}=8\sqrt{\pi}$. These will be used for the numerical calculations of the correlation functions a little later.

Before proceeding, we prescribe a nondimensionalization procedure which considerably simplifies the notation. All velocities are nondimensionalized by $\sqrt{\bar{T}}$, and all lengths are scaled by the mean free path $(\bar{\rho}d^{D-1})^{-1}$, where $\bar{\rho}$ is the mean number density. These are the relevant velocity and length scales in a dilute gas; the particle diameter enters the formulation only indirectly through the mean free path. Dimensional expressions for the transport coefficients can be recovered at a later time by restoring suitable powers of the length and velocity scales. The above equations (12)–(14) are linearized in the perturbations and transformed into Fourier space using the Fourier transform

$$\tilde{\star}(\mathbf{k})=\int d\mathbf{x}\,\exp(-\imath\mathbf{k}\cdot\mathbf{x})\star'(\mathbf{x}). \tag{18}$$

The inverse Fourier transform is defined as

$$\star'(\mathbf{x})=\int_{\mathbf{k}}\exp(\imath\mathbf{k}\cdot\mathbf{x})\tilde{\star}(\mathbf{k}), \tag{19}$$

where the short form $\int_{\mathbf{k}}$ is used for $(2\pi)^{-D}\int d\mathbf{k}$, where D is the dimensionality. The dispersion relations for the density, velocity, and temperature fields are

$$\frac{D\tilde{\rho}}{Dt}+\imath(k_x\tilde{u}_x+k_y\tilde{u}_y+k_z\tilde{u}_z)=0, \tag{20}$$

$$\frac{D\tilde{u}_x}{Dt}+\epsilon\dot{\gamma}\tilde{u}_y=-\bar{p}_{\rho}^{\dagger}\imath k_x\tilde{\rho}-\bar{p}^{\dagger}\imath k_x\tilde{T}-\bar{\mu}^{\dagger}k^2\tilde{u}_x-\bar{\zeta}k_x(k_x\tilde{u}_x+k_y\tilde{u}_y+k_z\tilde{u}_z)+(1/2)\epsilon\dot{\gamma}\bar{\mu}^{\dagger}\imath k_y\tilde{T}, \tag{21}$$

$$\frac{D\tilde{u}_y}{Dt}=-\bar{p}_{\rho}^{\dagger}\imath k_y\tilde{\rho}-\bar{p}^{\dagger}\imath k_y\tilde{T}-\bar{\mu}^{\dagger}k^2\tilde{u}_y+\bar{\zeta}k_y(k_x\tilde{u}_x+k_y\tilde{u}_y+k_z\tilde{u}_z)+(1/2)\epsilon\dot{\gamma}\bar{\mu}^{\dagger}\imath k_x\tilde{T}, \tag{22}$$

$$\frac{D\tilde{u}_z}{Dt}=-\bar{p}_{\rho}^{\dagger}\imath k_z\tilde{\rho}-\bar{p}^{\dagger}\imath k_z\tilde{T}-\bar{\mu}^{\dagger}k^2\tilde{u}_z+\bar{\zeta}k_z(k_x\tilde{u}_x+k_y\tilde{u}_y+k_z\tilde{u}_z), \tag{23}$$

$$C_v \frac{D\tilde{T}}{Dt} = -\bar{K}^{\dagger} k^2 \tilde{T} + 2\epsilon \bar{\mu}^{\dagger} \dot{\gamma} (\imath k_x \tilde{u}_y + \imath k_y \tilde{u}_x) + (1/2)\epsilon^2 \bar{\mu}^{\dagger} \dot{\gamma}^2 \tilde{T} - \epsilon^2 \bar{D}_{\rho}^{\dagger} \tilde{\rho} - (3/2)\epsilon^2 \bar{D}^{\dagger} \tilde{T}, \tag{24}$$

where $\bar{\zeta} = (\bar{\mu}_b^{\dagger} + \bar{\mu}^{\dagger}/3)$ and $(D/Dt) = (\partial/\partial t) + \epsilon \dot{\gamma} k_x (\partial/\partial k_y)$. Note that the wave vectors in the above equation are scaled by $\bar{\rho} d^{D-1}$, and time is scaled by $(\bar{T}^{1/2} \bar{\rho} d^{D-1})^{-1}$. The above equations contain derivatives with respect to the wave vector in the substantial derivative on the left-hand side. These can be simplified by taking into account the turning of the wave vector due to the mean flow. We define a time-dependent wave vector in the y direction as

$$k_y(t) = k_y(0) - \epsilon \dot{\gamma} t k_x, \tag{25}$$

while the other two components of the wave vector are time independent. When expressed in terms of the time-dependent wave vector, the substantial derivatives on the left-hand side of Eqs. (20)–(24) reduce to partial derivatives, thus removing all derivatives with respect to the wave number in the conservation equation. However, this simplification comes at a price, because the wave number is now a function of time. With the definition of a time-dependent wave vector, the conservation equations can be reduced to the form

$$\frac{\partial}{\partial t} \tilde{\mathbf{\Phi}} + \mathbf{L} \cdot \tilde{\mathbf{\Phi}} = 0, \tag{26}$$

where the 5×1 matrix ϕ is

$$\tilde{\mathbf{\Phi}} = \begin{pmatrix} \tilde{\rho} \\ \tilde{u}_x \\ \tilde{u}_y \\ \tilde{u}_z \\ \sqrt{C_v}\tilde{T} \end{pmatrix} \tag{27}$$

and the 5×5 dispersion matrix $\mathbf{L}$ is a function of the wave numbers and is also a function of time due to the dependence of the wave vector on time. Note that the eigenvectors $\tilde{\Phi}$ of the macroscopic fields correspond to an average over the distribution function of the eigenvectors of the microscopic conserved variables,

$$\tilde{\Phi}_I = \int_{\alpha} f_{\alpha} \phi_{\alpha I}, \tag{28}$$

for all values of I, where the elements $\phi_{\alpha I}$ are given in Eq. (10). The matrix $\mathbf{L}$ can be written as the sum of two parts,

$$\mathbf{L} = \mathbf{L}_{\text{elastic}} + \mathbf{L}_{\text{inelastic}}, \tag{29}$$

$\mathbf{L}_{\text{elastic}}$ being the hydrodynamic matrix for an elastic fluid, while $\mathbf{L}_{\text{inelastic}}$ is the additional contribution for an inelastic fluid. The two components are

$$\mathbf{L}_{\text{elastic}} = \begin{pmatrix} 0 & \imath k_x & \imath k_y & \imath k_z & 0 \\ \imath k_x & \bar{\mu}^{\dagger} k^2 + \bar{\zeta} k_x^2 & \bar{\zeta} k_x k_y & \bar{\zeta} k_x k_z & (\imath k_x/\sqrt{C_v}) \\ \imath k_y & \bar{\zeta} k_x k_y & \bar{\mu}^{\dagger} k^2 + \bar{\zeta} k_y^2 & \bar{\zeta} k_y k_z & (\imath k_y/\sqrt{C_v}) \\ \imath k_z & \bar{\zeta} k_x k_z & \bar{\zeta} k_y k_z & \bar{\mu}^{\dagger} k^2 + \bar{\zeta} k_z^2 & (\imath k_z/\sqrt{C_v}) \\ 0 & (\imath k_x/\sqrt{C_v}) & (\imath k_y/\sqrt{C_v}) & (\imath k_z/\sqrt{C_v}) & (\bar{K}^{\dagger} k^2/C_v) \end{pmatrix}, \tag{30}$$

$$\mathbf{L}_{\text{inelastic}} = \begin{pmatrix} 0 & 0 & 0 & 0 & 0 \\ -\imath \bar{\mu}_{\rho}^{\dagger} \dot{\gamma} k_y & 0 & \epsilon \dot{\gamma} & 0 & -(\imath \epsilon/2) \bar{\mu}^{\dagger} \dot{\gamma} k_y \\ -\imath \bar{\mu}_{\rho}^{\dagger} \epsilon \dot{\gamma} k_x & 0 & 0 & 0 & -[(\imath \epsilon/2) k_x \bar{\mu}^{\dagger} \dot{\gamma}] \\ 0 & 0 & 0 & 0 & 0 \\ (\epsilon^2/\sqrt{C_v})(\bar{D}_{\rho}^{\dagger} - \bar{\mu}_{\rho}^{\dagger} \dot{\gamma}^2) & (-2\imath k_y \epsilon \bar{\mu}^{\dagger} \dot{\gamma})/\sqrt{C_v} & (-2\imath k_x \epsilon \bar{\mu}^{\dagger} \dot{\gamma})/\sqrt{C_v} & 0 & \epsilon^2 (\bar{D}^{\dagger} - \bar{\mu}^{\dagger} \dot{\gamma}^2) \end{pmatrix}. \tag{31}$$

It should be noted that Eqs. (27), (30), and (31) are obtained for a three-dimensional system; the equivalent expressions for a two-dimensional system are obtained by removing the fourth element in Eq. (27) and the fourth row and column in Eqs. (30) and (31).

A. Hydrodynamic modes for $k \gg \epsilon$

The $O(\epsilon^0)$ solutions for the eigenvalues and eigenfunctions are identical to the decay rates of the conserved modes in a fluid of elastic particles. For an elastic system, there are two propagating modes, for which the imaginary part of the growth rate is proportional to k, while the real part is negative and proportional to k^2. The other three modes are diffusive, with real negative eigenvalues proportional to k^2. Of these two correspond to momentum diffusion perpendicular to the direction of the wave vector, while the other corresponds to thermal diffusion. Using an expansion in the parameter ϵ, the eigenvalues correct to $O(\epsilon)$ are

$$\lambda_1 = \imath c_s k + \frac{1}{2}[\Gamma k^2 + \epsilon\dot{\gamma}(k_x k_y/k^2)],$$

$$\lambda_2 = -\imath c_s k + \frac{1}{2}[\Gamma k^2 + \epsilon\dot{\gamma}(k_x k_y/k^2)],$$

$$\lambda_3 = \bar{\mu}^\dagger k^2 - (\epsilon\dot{\gamma}k_x k_y/2k^2),$$

$$\lambda_4 = \bar{\mu}^\dagger k^2,$$

$$\lambda_5 = \frac{\bar{K}^\dagger \bar{p}_\rho^\dagger k^2}{C_v c_s^2}, \tag{32}$$

where the speed of sound c_s is

$$c_s = \sqrt{\frac{\bar{p}^{\dagger 2} + \bar{p}_\rho^\dagger C_v}{C_v}} \tag{33}$$

and the sound damping constant Γ is

$$\Gamma = \frac{1}{2}\left(\frac{\bar{K}^\dagger(C_p - C_v)}{C_p C_v} + \bar{\zeta} + \frac{4\bar{\mu}^\dagger}{3}\right). \tag{34}$$

In Eq. (32), λ_1 and λ_2 are the growth rates of the propagating modes, λ_3 and λ_4 are the growth rates for the transverse momentum, and λ_5 is the growth rate for energy.

The calculation of the eigenfunctions of Eq. (26) is a little more complicated, because the matrix $\mathbf{L}$ is a function of time. Therefore, it is necessary to solve the implicit equation

$$\mathbf{LE} = \mathbf{E\Lambda} - \frac{\partial \mathbf{E}}{\partial t}, \tag{35}$$

where $\mathbf{E}$ is the $n \times n$ matrix of generalized eigenvectors of the matrix $\mathbf{L}$, which contains the eigenvectors as its columns, and $\mathbf{\Lambda}$ is the $n \times n$ diagonal matrix which contains the eigenvalues of $\mathbf{L}$ as its diagonal elements. If we insert Eq. (35) into the differential equation (26), we obtain

$$\frac{\partial}{\partial t}\tilde{\mathbf{\Xi}} + \mathbf{\Lambda}\tilde{\mathbf{\Xi}} = 0, \tag{36}$$

where the vector $\tilde{\mathbf{\Xi}}$ is related to the vector $\tilde{\mathbf{\Phi}}$ by

$$\tilde{\mathbf{\Xi}} = \mathbf{E}^{-1}\tilde{\mathbf{\Phi}}, \tag{37}$$

where $\tilde{\mathbf{\Phi}}$ is given in Eq. (27). Equation (36) can now be solved explicitly, since $\mathbf{\Lambda}$ is a diagonal matrix, and the variation of the density, velocity, and temperature with time can be obtained using Eq. (37). Equation (35) is best solved using an iterative procedure, which is outlined in the Appendix. This is designed to ensure that Eq. (35), which is a matrix equation, is a well-posed equation and satisfies all the solvability conditions. If we attempt to solve the matrix equation (35) as a set of differential equations, then the time derivative of one element of the matrix would depend on other elements, and it would be difficult to disentangle these and ensure that the solvability condition is satisfied. Using the expansion, we have ensured that the solvability conditions for both the diagonal and off-diagonal elements are satisfied at each order in the expansion, so that a solutions for the eigenfunctions exist and they are unique (subject to specified initial conditions).

B. Hydrodynamic modes for $k \ll \epsilon$

Implicit in the calculation of the eigenvalues (32) and eigenvectors (A7) has been the assumption that $\epsilon \ll k$. However, $\mathbf{k}$ is a variable in the above calculation and it varies from 0 to the upper cutoff (inverse of the microscopic scale). One important wave vector domain, from the perspective of the present calculation, is the limit $k \to 0$ at finite but small ϵ. Note that the first correction to the eigenvalues λ_1, λ_2, and λ_4 is proportional to ϵ and this correction becomes large compared to the leading-order solution for $k \ll \epsilon$. In addition, the first correction to the eigenvectors in Eqs. (A8) and (A9) is $O(\epsilon/k)$ in the small-wave-number limit and this term becomes large compared to the leading-order contribution for $k \ll \epsilon$. The procedure adopted to obtain the eigenvalues (32) was to first expand in k after setting $\epsilon = 0$, to calculate the leading-order solutions, and then to insert these into the governing equations to obtain the first correction. For the limit $k \ll \epsilon$, it is necessary to first take the limit $k \to 0$ at a fixed value of ϵ and then expand the solutions in a series in ϵ. This procedure is outlined in the reminder of this section.

This expansion is facilitated by realizing that for $k \ll \epsilon$, the rate of conduction of energy in the energy balance equation (proportional to k^2), is small compared to the rates of production and dissipation (proportional to ϵ^2). In this case, energy is no longer a conserved variable and the temperature perturbations are enslaved to the density and the velocity perturbations. This can be understood by returning to examine the energy balance equation for the fluctuations, Eq. (24), in the limit $k \to 0$. If we retain only linear terms in the equation, we obtain

$$C_v \frac{\partial \tilde{T}}{\partial t} = [(1/2)\epsilon^2 \bar{\mu}^\dagger \dot{\gamma}^2 - (3/2)\epsilon^2 \bar{D}^\dagger]\tilde{T} - \epsilon^2 \bar{D}_\rho^\dagger \tilde{\rho}. \tag{38}$$

From energy balance for the mean flow, the rates of shear production and inelastic dissipation are related by $\bar{\mu}^\dagger \dot{\gamma}^2 = \bar{D}^\dagger$. Therefore, the energy balance equation (38) reduces to

$$C_v \frac{\partial \tilde{T}}{\partial t} + \epsilon^2 \bar{D}^\dagger \tilde{T} = -\epsilon^2 \bar{D}_\rho^\dagger \tilde{\rho}. \tag{39}$$

The above equation can be solved to obtain $\tilde{T}$ as a function of $\tilde{\rho}$ in the limit $k \ll \epsilon$:

$$\tilde{T}(t) = \exp(-s_T t)\tilde{T}(0) + \int_0^t dt' \exp[-s_T(t-t')] \times [-C_v^{-1}\epsilon^2 \bar{D}_\rho^\dagger \tilde{\rho}(t')], \tag{40}$$

where the relaxation rate s_T for the temperature fluctuations is given by $(\epsilon^2 \bar{D}^\dagger / C_v)$. It should be noted, from Eq. (40), that the relaxation rate for temperature fluctuations is finite and does not decay to zero in the limit $k \to 0$. This is because energy is a nonconserved (fast) variable in this limit. In contrast, the relaxation rate for the density fluctuations does go

to zero in the limit $k \to 0$ and the results obtained a little later in Eq. (44) below indicates that it decreases proportional to $k^{2/3}$. Therefore, the relaxation rate for the energy fluctuations is fast compared to that for density fluctuations in the limit $k \to 0$.

When the relaxation rate for temperature fluctuations is fast compared to that for density fluctuations, Eq. (40) can be simplified when we are considering time scales comparable to the time scale for density fluctuations (the slow time). Over time scales comparable to the relaxation time of the density fluctuations, $s_T t \gg 1$, because the relaxation time for density fluctuations is large compared to s_T^{-1}. In this case, the first term on the right-hand side of Eq. (40) is negligible. In the second term on the right, we use a Taylor series expansion in time for $\tilde{\rho}$ to obtain

$$\begin{aligned}\tilde{T}(t) &= -\frac{\epsilon^2 \bar{D}_\rho^\dagger}{C_v}\int_0^t dt' \exp(-s_T(t-t'))\left(\tilde{\rho}(t) + (t'-t)\left.\frac{d\tilde{\rho}(t^*)}{dt^*}\right|_{t^*=t} + \frac{(t'-t)^2}{2}\left.\frac{d^2\tilde{\rho}(t^*)}{dt^{*2}}\right|_{t^*=t} + \cdots\right) \\ &= -\frac{\epsilon^2 \bar{D}_\rho^\dagger}{C_v}\left(\tilde{\rho}(t)\int_0^t dt' \exp[-s_T(t-t')] + \left.\frac{d\tilde{\rho}(t^*)}{dt^*}\right|_{t^*=t}\int_0^t dt(t'-t)\exp[-s_T(t-t')] + \left.\frac{d^2\tilde{\rho}(t^*)}{dt^{*2}}\right|_{t^*=t}\right. \\ &\quad \left.\times\int_0^t dt\frac{(t'-t)^2}{2}\exp[-s_T(t-t')] + \cdots\right). \end{aligned} \tag{41}$$

When the relaxation time for density perturbations is large compared to that for temperature relaxation—that is, $s_T t \gg 1$—the terms proportional to $\exp(-s_T t)$ can be neglected in Eq. (41) and the result is

$$\tilde{T}(t) = -\frac{\epsilon^2 \bar{D}_\rho^\dagger}{C_v}\left(\frac{\tilde{\rho}(t)}{s_T} + \frac{1}{s_T^2}\left.\frac{d\tilde{\rho}(t^*)}{dt^*}\right|_{t^*=t} + \frac{1}{s_T^3}\left.\frac{d^2\tilde{\rho}(t^*)}{dt^{*2}}\right|_{t^*=t} + \cdots\right). \tag{42}$$

Since the perturbation to the density changes over a time scale large compared to s_T^{-1}, the first term on the right in Eq. (42) is the largest term and the others can be neglected. In this case, the equation for the temperature perturbation is

$$\tilde{T}(t) = -\frac{\epsilon^2 \bar{D}_\rho^\dagger C_v^{-1}\tilde{\rho}}{s_T} = -\frac{\bar{D}_\rho^\dagger \tilde{\rho}}{\bar{D}^\dagger} = -2\tilde{\rho}, \tag{43}$$

where the last step follows from the relation $\bar{D}_\rho^\dagger = 2\bar{D}^\dagger$ because the rate of dissipation of energy is proportional to ρ^2 in the dilute limit. It should be noted that Eq. (43) does not imply that temperature has the same relaxation rate as density or that temperature is a slow variable. On the contrary, Eq. (43) was obtained as an approximation of Eq. (40) in the limit where the relaxation rate for the temperature is fast compared to that for the density perturbations, so that the temperature perturbation relaxes to the value required to satisfy the right side of Eq. (39) over a short time comparable to the inverse of the relaxation rate s_T. Finally, it should be noted that Eq. (43) is an approximation correct to leading order in the limit $k \to 0$; there are higher corrections which are incorporated in the calculation when we evaluate the higher-order contributions to the eigenvalues, but these are not specified here.

The four solutions for the eigenvalues of the hydrodynamic matrix, obtained using an expansion in k in the limit $k \ll \epsilon$, are as follows:

$$\begin{aligned}\lambda_1 &= k^{2/3}s_0 + \frac{k^{4/3}}{3s_0}[1 + \epsilon\dot{\gamma}(k_x k_y/k^2)(\bar{\zeta} - 2\bar{\mu}^\dagger)] + \frac{k^2(\bar{\zeta} + 2\bar{\mu}^\dagger)}{3}, \\ \lambda_2 &= (-1)^{2/3}k^{2/3}s_0 + \frac{k^{4/3}}{3(-1)^{2/3}s_0}[1 + \epsilon\dot{\gamma}(k_x k_y/k^2)(\bar{\zeta} - 2\bar{\mu}^\dagger)] \\ &\quad + \frac{k^2(\bar{\zeta} + 2\bar{\mu}^\dagger)}{3}, \\ \lambda_2 &= (-1)^{4/3}k^{2/3}s_0 + \frac{k^{4/3}}{3(-1)^{4/3}s_0}[1 + \epsilon\dot{\gamma}(k_x k_y/k^2)(\bar{\zeta} - 2\bar{\mu}^\dagger)] \\ &\quad + \frac{k^2(\bar{\zeta} + 2\bar{\mu}^\dagger)}{3}, \\ \lambda_4 &= \bar{\mu}^\dagger k^2, \end{aligned} \tag{44}$$

where

$$\begin{aligned} &k^2 s_0^3 - \epsilon k_x k_y[(\bar{D}_\rho^\dagger \bar{p}^\dagger/\bar{\mu}^\dagger\dot{\gamma}) - (\bar{p}^\dagger\bar{\mu}_\rho^\dagger\dot{\gamma}/\bar{\mu}^\dagger) - \bar{p}_\rho^\dagger\dot{\gamma}] \\ &\quad - \epsilon^2 k_x^2[(3\bar{\mu}_\rho^\dagger\dot{\gamma}^2/2) - (\bar{D}_\rho^\dagger/2)] = 0. \end{aligned} \tag{45}$$

For a dilute granular gas, in the near elastic limit, using the numerical coefficients provided after Eq. (17), the equation for s_0 is

$$k^2 s_0^3 - \epsilon k_x k_y \dot{\gamma} + \epsilon^2 k_x^2 \bar{\mu}^\dagger \dot{\gamma}^2 = 0. \tag{46}$$

The fifth eigenvalue, which corresponds to energy fluctuations, has a finite value s_T in the limit $k \to 0$, as given in Eq. (40).

It is of interest to examine whether the eigenvalues calculated in Eq. (44) are unchanged by a reduction of the type given in Eq. (43)—that is, whether the eigenvalues of the conserved modes obtained using the reduction in Eq. (43) are identical to those which would have been obtained using the complete hydrodynamic matrix in Eqs. (30) and (31). This issue has been examined earlier by the author [14], and it has been found, by numerical solution of the complete hydrodynamic equations (30) and (31), that the leading-order solutions for the eigenvalues for the conserved modes are identical to those obtained using a reduction of the type given in Eq. (43) in the limit $k \ll \epsilon$. In addition, the transition from the regime $k \gg \epsilon$ (where it is appropriate to treat energy as a conserved variable) to the regime $k \ll \epsilon$ (where it is appropriate to treat energy as a nonconserved variable) has also been studied by a numerical solution of the complete hydrodynamic equations.

There are several important aspects of the eigenvalues in Eqs. (44) which merit further discussion.

(i) There are three coupled modes, whose growth rate is proportional to $k^{2/3}$ in the small-k limit. These correspond to a combination of the density, the longitudinal momentum, and the transverse momentum in the plane of shear. The fourth mode, which is diffusive, has the same growth rate as that for the transverse shear modes in an elastic fluid; from the eigenvector for this mode evaluated a little later, it can be inferred that this mode corresponds to the transverse momentum in the velocity-vorticity plane.

(ii) The three coupled modes s_1, s_2, and s_3 have contributions proportional to $k^{2/3}$, $k^{4/3}$, and k^2 in the limit $k \to 0$.

(iii) For the three coupled modes, the leading-order growth rates have equal magnitudes and their values are rotated by an angle $2\pi/3$ in the complex plane. If s_0 is positive, then there is one mode with growth rate on the positive real axis which grows exponentially at short time, while the other two modes decay exponentially and oscillate at short times. If s_0 is negative, there is one mode on the negative real axis which decays exponentially, while the other two have positive real components and exhibit an oscillatory growth.

(iv) However, it turns out that the contribution proportional to k^2 is always negative, and so this damps out perturbations in the long-time limit in a rotating reference frame in which the wave vector is given by Eq. (25).

(v) The $k^{2/3}$ behavior of the growth rate can be justified as follows. If we retain terms up to leading order in $O(k)$ and $O(\epsilon)$, the mass and momentum conservation equations reduce to

$$\partial_t \tilde{\rho} + \imath k_x \tilde{u}_x + \imath k_y \tilde{u}_y + \imath k_z \tilde{u}_z = 0, \tag{47}$$

$$\partial_t \tilde{u}_x + \epsilon \dot{\gamma} \tilde{u}_y + [-(2\bar{p}^\dagger - \bar{p}_\rho^\dagger)\imath k_x + \imath \epsilon \dot{\gamma} k_y \bar{\mu}^\dagger]\tilde{\rho} = 0, \tag{48}$$

$$\partial_t \tilde{u}_y + [-(2\bar{p}^\dagger - \bar{p}_\rho^\dagger)\imath k_y + \imath \epsilon \dot{\gamma} k_x \bar{\mu}^\dagger]\tilde{\rho} = 0, \tag{49}$$

$$\partial_t \tilde{u}_z - \imath k_z (2\bar{p}^\dagger - \bar{p}_\rho^\dagger)\tilde{\rho} = 0. \tag{50}$$

From the above equation, the dispersion relation for the eigenvalues λ can easily be obtained as

$$\lambda^3 + \lambda^2 D_2 + \lambda D_1 + D_0 = 0, \tag{51}$$

where the coefficients in the dispersion relation are

$$D_2 = -(2\bar{\mu}^\dagger + \bar{\zeta})k^2,$$

$$D_1 = -[k^2(2\bar{p}^\dagger - \bar{p}_\rho^\dagger) - k_x k_y \epsilon \dot{\gamma}(2\bar{\mu}^\dagger - \bar{\zeta})],$$

$$D_0 = -\epsilon \dot{\gamma}[k_x k_y (2\bar{p}^\dagger - \bar{p}_\rho^\dagger) - k_x^2 \epsilon \dot{\gamma} \bar{\mu}^\dagger]. \tag{52}$$

It is easy to verify that there are three solutions for the growth rates of the above equations which are proportional to $k^{2/3}$ in the limit $k \to 0$, and the solutions for these three are the leading-order solutions in Eqs. (44).

In fact, the $k^{2/3}$ behavior results from a coupling between the density and the x and y momentum equations in Eqs. (47)–(49). If we retain only the time derivatives and the terms that are lowest order in the wave number in these equations, we obtain, for perturbations along the x-y plane,

$$\partial_t \tilde{\rho} + \imath k_x \tilde{u}_x + \imath k_y \tilde{u}_y = 0, \tag{53}$$

$$\partial_t \tilde{u}_x + \epsilon \dot{\gamma} \tilde{u}_y = 0, \tag{54}$$

$$\partial_t \tilde{u}_y + [-(2\bar{p}^\dagger - \bar{p}_\rho^\dagger)\imath k_y + \imath \epsilon \dot{\gamma} k_x \bar{\mu}^\dagger]\tilde{\rho} = 0. \tag{55}$$

In the above equations, the streamwise velocity $\tilde{u}_x$ is coupled to the cross-stream velocity $\tilde{u}_y$ only due to the advection term caused by the mean flow. Therefore, pressure and viscous effects are small in the x momentum equation to leading order in the wave number, so the rate of change of momentum in the x direction is due to advection alone. In the y direction, the rate of change of momentum is due to the dependence of the pressure and viscosity on the density. If we combine Eqs. (54) and (55), we obtain the x momentum equation as

$$\frac{\partial^2 \tilde{u}_x}{\partial t^2} + \epsilon \dot{\gamma}[-(2\bar{p}^\dagger - \bar{p}_\rho^\dagger)\imath k_y + \imath \epsilon \dot{\gamma} k_x \bar{\mu}^\dagger]\tilde{\rho} = 0 \tag{56}$$

and we obtain a third-order equation for the density of the form

$$\frac{\partial^3 \tilde{\rho}}{\partial t^3} + \epsilon \dot{\gamma}[-(2\bar{p}^\dagger - \bar{p}_\rho^\dagger)k_x k_y + \epsilon^2 \dot{\gamma}^2 k_x^2 \bar{\mu}^\dagger]\tilde{\rho} = 0. \tag{57}$$

Clearly, the above equation provides a growth rate that scales as $k^{2/3}$. The critical difference between a sheared and an unsheared fluid is that there is the advective term in the x momentum equation of a sheared fluid that is independent of k in the limit $k \to 0$; in contrast, in an unsheared fluid, the coefficients of all terms (apart from the time derivative) are $O(k)$ or $O(k^2)$. Due to the advective term, the coefficient of the second term on the left-hand side of Eq. (57) is k^2; in contrast, the coefficient would be k^3 or a higher power of k if all terms in the matrix had coefficients of $O(k)$ or $O(k^2)$. Therefore, we find that the growth rate is proportional to $k^{2/3}$ for $k \to 0$.

C. Modes with $k_x=0$

It should be noted that the solutions for the eigenvalues in Eqs. (44) are not valid for $k_x \to 0$. This is because s_0 goes to zero in this limit and the $O(k^{4/3})$ corrections to $\lambda_1-\lambda_3$ diverge. The origin of the singularity can be traced back to the leading-order solution of the dispersion relation (51), where we had neglected the second and third terms proportional to s^2 and s, respectively, on the left-hand side, since these are subdominant for $s \sim k^{2/3}$. For $k_x=0$, we find that the fourth term on the left is also equal to zero, resulting in the solution $s_0=0$ in Eqs. (44). In order to rectify this, it is necessary to return to the hydrodynamic matrix, Eqs. (30) and (31), and set $k_x=0$. The resulting dispersion matrix is solved in order to obtain the growth rates as a function of k_y and k_z. The solutions obtained in this manner, correct to $O(k^2)$, are

$$\lambda_1 = + \sqrt{\left(-2\bar{p}^\dagger k_y^2 + \frac{(k_y^2+k_z^2)[\bar{D}_\rho^\dagger \bar{p}^\dagger - \dot{\gamma}^2(\bar{p}_\rho^\dagger \bar{\mu}^\dagger + \bar{\mu}_\rho^\dagger \bar{p}^\dagger)]}{\bar{\mu}^\dagger \dot{\gamma}^2} \right)},$$

$$\lambda_1 = - \sqrt{\left(-2\bar{p}^\dagger k_y^2 + \frac{(k_y^2+k_z^2)[\bar{D}_\rho^\dagger \bar{p}^\dagger - \dot{\gamma}^2(\bar{p}_\rho^\dagger \bar{\mu}^\dagger + \bar{\mu}_\rho^\dagger \bar{p}^\dagger)]}{\bar{\mu}^\dagger \dot{\gamma}^2} \right)},$$

$$\lambda_3 = -\bar{\mu}^\dagger (k_y^2+k_z^2),$$

$$\lambda_4 = -\bar{\mu}^\dagger (k_y^2+k_z^2). \tag{58}$$

The roots λ_1 and λ_2 are imaginary for $k_z=0$—i.e., for perturbations along the gradient direction—indicating that there are propagating modes in this direction, which are stabilized by viscous effects. In three dimensions, there is one unstable and one stable mode for perturbations in the vorticity direction ($k_x=k_y=0$). The solutions (58) are applicable only in the wave number domains where they are large compared to the solutions (45). It is easily verified that λ_1 and λ_2 in Eq. (58) are larger than the equivalent solutions in Eq. (45) only for $k_x^{1/3}k_y^{1/3} < \sqrt{k_y^2+k_z^2}$ or for $\hat{k}_x < k$, where $\hat{k}_x$ is the x component of the unit vector $\hat{\mathbf{k}}$ along the direction of the wave vector $\mathbf{k}$. Similarly, the solution λ_3 in Eqs. (58) is larger than the equivalent solution in (45) only for $k_x^{1/3}k_y^{1/3} < (k_y^2+k_z^2)$ or for $\hat{k}_x < k$[4]. The eigenvectors corresponding to the eigenvalues (58) can be easily evaluated correct to leading order in an expansion in the wave number:

$$\mathbf{E} = \left[\begin{pmatrix} 0 \\ \lambda_1 \\ \epsilon\dot{\gamma} \\ 0 \end{pmatrix} \begin{pmatrix} 0 \\ \lambda_2 \\ \epsilon\dot{\gamma} \\ 0 \end{pmatrix} \begin{pmatrix} 0 \\ 0 \\ -k_z \\ k_y \end{pmatrix} \begin{pmatrix} 1 \\ 0 \\ 0 \\ 0 \end{pmatrix} \right]. \tag{59}$$

This completes the calculation of the eigenvalues and eigenvectors of the hydrodynamic equations for both $k \gg \epsilon$ (where energy is a conserved variable) and $k \ll \epsilon$ (where energy is treated as a nonconserved variable). In Part II, we will calculate the renormalization of the transport coefficients from the ring-kinetic equation using these hydrodynamic modes. Before this, we analyze the autocorrelation functions for the conserved variables in a linear shear flow.

D. Time correlation functions

The time correlation functions of the conserved variables are evaluated in the present section in order to illustrate the differences between an elastic fluid and a sheared inelastic fluid. In an elastic fluid, there are five conserved modes: the density, the three components of the momentum, and the energy. The eigenvalues for these modes are given in Eq. (32) with $\epsilon=0$, while the eigenfunctions are given in Eqs. (A7) and (A8) in the Appendix. For a sheared inelastic fluid with $k \ll \epsilon$, there are four hydrodynamic modes: the mass and the three components of the momentum. Energy is not conserved, since there is a local balance between the rates of production and dissipation of energy. The eigenvalues in this case are given by Eqs. (44), and the eigenfunctions are given by Eqs. (A10) and (58). If we know the initial value of the set of hydrodynamic variables at the initial time $t=0$, then the system can be propagated forward in time to determine the values of the hydrodynamic variables at a later time t, using the eigenvalues and eigenvectors derived here. So the value of any of the hydrodynamic variables $\tilde{\Phi}_I$ in Eq. (27), at time t, can be written as

$$\tilde{\Phi}_I(\mathbf{k}(t),t) = E_{IK}(\mathbf{k}(t),t)\tilde{\xi}_K(\mathbf{k}(t),t), \tag{60}$$

where $\tilde{\xi}(k(t),t)$ is defined in Eq. (37) and $\mathbf{E}$, the array of eigenvectors, are defined in the Appendix in Eqs. (A7) and (A8) for $k \gg \epsilon$ and in Eqs. (A10) and (A11) for $k \ll \epsilon$. The functions $\tilde{\xi}_K(k(t),t)$ satisfy Eq. (36), where $\mathbf{\Lambda}$ is a diagonal matrix. Therefore, the time propagation of $\tilde{\xi}_K(k(t),t)$ can be expressed as

$$\begin{aligned}\tilde{\xi}_K(\mathbf{k}(t),t) &= \exp\left(\int_0^t dt' \lambda_K(\mathbf{k}(t'),t') \right) \tilde{\xi}_K(\mathbf{k}(0),0) \\ &= \exp\left(\int_0^t dt' \lambda_K(\mathbf{k}(t'),t') \right) E_{KL}^{-1}(\mathbf{k}(0)) \tilde{\Phi}_L(\mathbf{k}(0),0),\end{aligned} \tag{61}$$

where the function $\tilde{\xi}_K(k(0),0)$ is once again be expressed in terms of $\tilde{\Phi}_L(k(0),0)$ using Eq. (37). Inserting Eq. (61) into Eq. (60), we obtain evolution equation for $\tilde{\Phi}_I(k(t),t)$ as

$$\begin{aligned}\tilde{\Phi}_I(\mathbf{k}(t),t) = E_{IK}(\mathbf{k}(t),t) &\exp\left(\int_0^t dt' \lambda_K(\mathbf{k}(t'),t') \right) \\ &\times E_{KL}^{-1}(\mathbf{k}(0),0) \tilde{\Phi}_L(\mathbf{k}(0),0).\end{aligned} \tag{62}$$

The time correlation for Φ_I can be written, using Eq. (62), as

$$\langle \tilde{\Phi}_I(\mathbf{k}(t),t)\tilde{\Phi}_J(\mathbf{k}'(0),0)\rangle = \langle E_{IK}(\mathbf{k}(t),t)\tilde{\xi}_K(\mathbf{k}(t),t)\tilde{\Phi}_J(\mathbf{k}'(0),0)\rangle$$
$$= \left\langle E_{IK}(\mathbf{k}(t),t)\exp\left(\int_0^t dt'\lambda_K(\mathbf{k}(t'),t')\right)\tilde{\xi}_K(\mathbf{k}(0),0)\tilde{\Phi}_J(\mathbf{k}'(0),0)\right\rangle$$
$$= E_{IK}(\mathbf{k}(t),t)\exp\left(\int_0^t dt'\lambda_K(\mathbf{k}(t'),t')\right)E^{-1}_{KL}(\mathbf{k}(0),0)\langle\tilde{\Phi}_L(\mathbf{k}(0),0)\tilde{\Phi}_J(\mathbf{k}'(0),0)\rangle$$
$$= E_{IK}(\mathbf{k}(t))\exp\left(\int_0^t dt'\lambda_K(\mathbf{k}(t'),t')\right)E^{-1}_{KL}\delta(\mathbf{k}(0)+\mathbf{k}'(0))\,\delta_{LJ}, \tag{63}$$

where $\tilde{\xi}_K$ is the Kth component of the vector $\tilde{\Xi}$ in Eq. (37) and $\langle\tilde{\Phi}_L(k(0),0)\tilde{\Phi}_J(k'(0),0)\rangle$ represents the equal-time correlation function. Since the basis functions $\tilde{\Phi}_I$ are defined to be orthonormal, the equal-time correlation function is an identity matrix. In the above equation, capital subscripts are used to denote the components of a matrix and repeated indices denote a summation. In the leading approximation, where the distribution function is a Maxwell-Boltzmann distribution, the equal-time correlation function matrix is an identity matrix, since the functions ϕ_I are normalized. Using this and from a knowledge of the eigenvalues λ_K and eigenvectors E_{IK}, the autocorrelation functions can be obtained. We do not provide the details, because the algebra is tedious but straightforward. The final results for the autocorrelation functions for the velocity in the flow and gradient directions, in the leading approximation in small ϵ, are

$$\langle\tilde{u}_x(\mathbf{k}(t),t)\tilde{u}_x(-\mathbf{k}(0),0)\rangle = (1/3)\{\exp(-S_0-S_1-S_2)$$
$$+\exp[(-1)^{2/3}S_0+(-1)^{4/3}S_1+S_2]$$
$$+\exp[(-1)^{4/3}S_0+(-1)^{2/3}S_1+S_2]\}$$

$$\langle\tilde{u}_y(\mathbf{k}(t),t)\tilde{u}_y(-\mathbf{k}(0),0)\rangle$$
$$=[s_0(\mathbf{k}(0))/3s_0(\mathbf{k}(t))]\{\exp(-S_0-S_1-S_2)$$
$$+\exp[(-1)^{2/3}S_0+(-1)^{4/3}S_1+S_2]$$
$$+\exp[(-1)^{4/3}S_0+(-1)^{2/3}S_1+S_2]\},$$

$$\langle\tilde{u}_z(\mathbf{k}(t),t)\tilde{u}_z(-\mathbf{k}(0),0)\rangle = \exp(-\bar{\mu}^{\dagger}dk^2t) \tag{64}$$

where s_0 is given as a function of $k(t)$ in Eq. (45) and

$$S_0(t) = \int_0^t dt' s_0(t'),$$

$$S_1(t) = \int_0^t dt' \frac{1}{3s_0(t')}[k(t')^2 + \epsilon\dot{\gamma}k_xk_y(t')(\bar{\zeta}-2\bar{\mu}^{\dagger})],$$

$$S_2(t) = \int_0^t dt' \frac{k(t')^2(\bar{\zeta}+2\bar{\mu}^{\dagger})}{3}, \tag{65}$$

and $k_y(t)$ is given in Eq. (25). It should be noted that the correlation functions in Eqs. (64) are the largest contributions in the limit $k\to 0$, and there are additional terms which are higher order in k not included in Eqs. (64).

The decay of the z component of the velocity autocorrelation function in Eqs. (64) is the same as that in an elastic fluid, and so we do not examine this further. The Fourier transforms of the velocity autocorrelation functions in the flow and gradient directions, $\langle u_x(k(t),t)u_x(-k(0),0)\rangle$ and $\langle u_y(k(t),t)u_y(-k(0),0)\rangle$, are shown as a function of time for specific values of the wave numbers k_x and k_y in Fig. 1. It should be noted that this calculation, using Eqs. (64), is correct only to leading order in the parameter ϵ. In addition, this

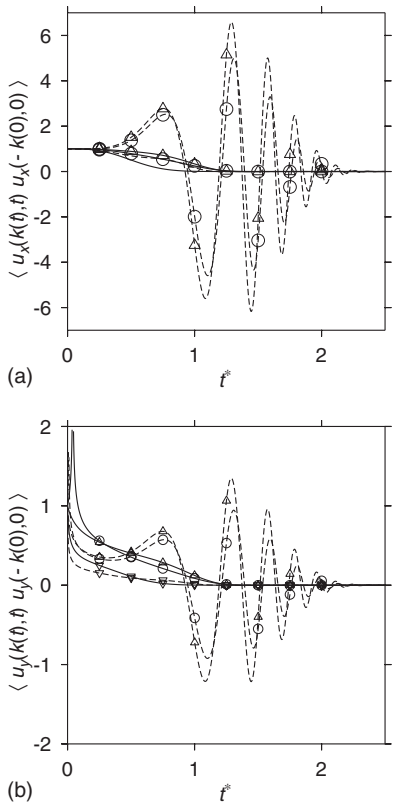

FIG. 1. The scaled Fourier transform of the velocity autocorrelation function, $\langle u_x(k(t),t)u_x(-k(0),0)\rangle$ (a) and $\langle u_y(k(t),t)\times u_y(-k(0),0)\rangle$ (b) as a function of scaled time $t^*=t\epsilon\dot{\gamma}k^{2/3}$ for $\epsilon=0.1$, $k=0.01$ (solid line) and $k=0.001$ (dashed line), for $\hat{k}_x=(1/\sqrt{2})$, $\hat{k}_y=(1/\sqrt{2})$ (○); $\hat{k}_x=(1/\sqrt{2})$, $\hat{k}_y=(-1/\sqrt{2})$ (△); $\hat{k}_x=1$, $\hat{k}_y=0$ (▽).

calculation is carried out using a time-dependent wave vector k, as shown in Fig. 1. In Fig. 1(b) for the velocity autocorrelation function in the gradient direction, the initial sharp increase is because of the factor $s_0(k(t))$ in the denominator of Eqs. (64) is going through zero. This is an artifact of our use of the leading-order approximation for the eigenvalue matrix in Eqs. (64); a more careful analysis would involve a matched asymptotic approximation in which a different approximation is used for the regions where $s_0(k(t))$ passes through zero. However, the singularity is integrable, since $s_0(k(t)) \sim t^{1/3}$, and so we do not use a more refined approximation here.

There are several interesting features in Fig. 1. The first is that there are large fluctuations in the autocorrelation function for u_x. In contrast to an equilibrium fluid, where the autocorrelation function has a maximum value of 1 at $t=0$, the autocorrelation function has a magnitude larger than 1 in the present case. This is because, as noted below Eq. (45), there are one or two unstable modes at short time in the present system, which cause a transient growth of perturbations in a reference frame rotating with the wave vector. In addition, two of the roots for the growth rate have imaginary parts, leading to the oscillatory nature of the autocorrelation function. It is important to note that the amplitude of fluctuations increases as the wave number is decreased, indicating that the modes that experience the largest transient growth are those with the largest wavelength. There are oscillations in the autocorrelation function for u_y as well, but these are much smaller in magnitude. This indicates that the fluctuations are highly anisotropic, with the fluctuations in the flow direction having the largest magnitude in the long-wave limit.

In order to quantify the growth of fluctuations, we can define an integral time for the decay of fluctuations as

$$I_{ij}(\mathbf{k}) = \int_0^\infty dt \langle u_i(\mathbf{k}(t),t) u_j(-\mathbf{k}(0),0)\rangle. \tag{66}$$

The integral times for the fluctuations in the flow and gradient directions are shown in Fig. 2. It is obvious that the integral time is the largest for the fluctuations in the flow directions, while that for fluctuations in the gradient direction is much smaller. The scaling for the integral time in the limit $k \to 0$ can be inferred as follows. Naively, we would expect the fluctuation amplitude to attain a maximum for $k^{2/3}t \gg k^2t^3$, because s_0 in Eqs. (44) is proportional to $k^{2/3}$ in the short-time limit, whereas the decay rates are proportional to $\dot{\gamma}^2k^2t^2$ in the long-time limit in Eqs. (44). This balance would give $I_{xx} \propto k^{-2/3}$ for $k \to 0$. However, the autocorrelation functions in Fig 2 shows an increase closer to $k^{-4/5}$. This is because s_0 in Eq. (45) contains a contribution proportional to $(k_xk_y)^{1/3}$, which is increasing with time due to the linear increase of k_y with time in Eq. (25). Therefore, the initial growth rate is proportional to $k^{2/3}t^{1/3}$, while the decay rate in the long-time limit is proportional to k^2t^2. A balance between these two provides the scaling $I_{xx} \propto k^{-4/5}$, as observed in Fig. 2. The integral time I_{yy} shows a smaller increase, because the magnitude of the autocorrelation function does not show large fluctuations in Fig. 1, but this is also consistent with the $k^{-4/5}$ scaling law.

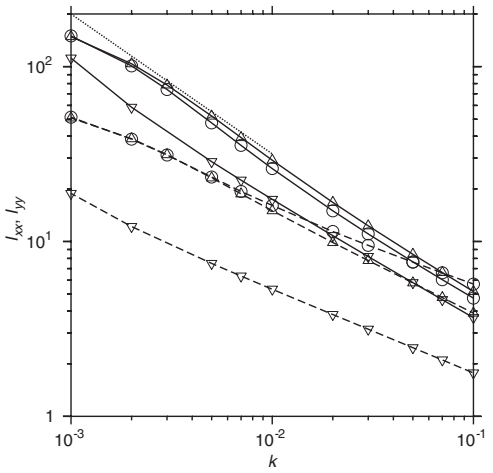

FIG. 2. The integral times I_{xx} (solid lines) and I_{yy} (dashed lines) as a function of wave number k for $\hat{k}_x=(1/\sqrt{2})$, $\hat{k}_y=(1/\sqrt{2})$ (○); $\hat{k}_x=(1/\sqrt{2})$, $\hat{k}_y=(-1/\sqrt{2})$ (△); $\hat{k}_x=1$, $\hat{k}_y=0$ (▽). The dotted line shows a slope of $-4/5$.

The long-time decay of the velocity autocorrelation function can be determined by inverting the Fourier transform shown in Fig. 2. We do not carry out the above integrals numerically, but rather restrict our attention to determining the scaling of the autocorrelation functions in the long-time limit. For the purposes of the calculation, we can divide the wave number space into two domains: the first for $k_x \sim 1$ where the growth rates of the hydrodynamic modes are given by Eq. (45) and the second along the gradient-vorticity plane where $k_x \to 0$, and the solutions for the growth rate are given by Eq. (58). In the first region, the dominant terms in the exponentials in Eqs. (64) have the asymptotic behavior $\exp(\text{const} \times k^{2/3}t^{4/3})$ in the short-time limit and $\exp(-\bar{\mu}^\dagger\dot{\gamma}^2k^2t^3)$ in the long-time limit, where const is a constant. Due to the rapid decay in the long-time limit, an estimate of the integral over the wave number can be obtained by using the short-time limit and cutting off the integral at the point where there is a crossover. There is a crossover between these two limiting behaviors for $k \sim (\dot{\gamma}t)^{-5/4}$, as shown in Fig. 2. If we use this crossover as the cutoff, it can easily be verified that

$$\langle u_x(\mathbf{x}(t),t) u_x(\mathbf{x}(0),0)\rangle \sim (\dot{\gamma}t)^{-5D/4}. \tag{67}$$

In three dimensions, the growth rate perpendicular to the plane of flow, λ_4 in Eq. (45), is proportional to k^2. In this case, the decay of the Fourier transform of the autocorrelation function for the velocity component u_z decays proportional to $\exp(-\bar{\mu}^\dagger k^2 t)$ at short time and proportional to $\exp(-(\bar{\mu}^\dagger k^2\dot{\gamma}^2t^3/3)$ in the long-time limit; there is no crossover in wave number space in this case. Therefore, the autocorrelation function for the component u_z also has the decay

$$\langle u_z(\mathbf{x}(t),t) u_z(\mathbf{x}(0),0)\rangle \sim (\dot{\gamma}t)^{-3D/2} \tag{68}$$

in the long-time limit.

The estimation in Eq. (67) has not incorporated the domains in wave number space where the decay rate is given by Eq. (58). These can be estimated as follows. If we use Eq. (63) for the autocorrelation function, along with Eqs. (58) and (59) for the growth rates and eigenvectors, we obtain the following expressions for the Fourier transforms of the autocorrelation functions:

$$\langle \tilde{u}_x(\mathbf{k}(t),t)\tilde{u}_x(-\mathbf{k}(0),0)\rangle = (1/2)[\exp(\lambda_1 t) + \exp(\lambda_2 t)],$$

$$\langle \tilde{u}_y(\mathbf{k}(t),t)\tilde{u}_y(-\mathbf{k}(0),0)\rangle = (1/2)[\exp(\lambda_1 t) + \exp(\lambda_2 t)],$$

$$\langle \tilde{u}_z(\mathbf{k}(t),t)\tilde{u}_z(-\mathbf{k}(0),0)\rangle = \exp[-\bar{\mu}(k_y^2 + k_z^2)t]. \quad (69)$$

The value of the autocorrelation function is obtained by integrating the above functions over the wave number space over which these are the dominant terms. The autocorrelation functions in the x and y directions are proportional to $\int_{\mathbf{k}} \exp(\pm \text{const} \times \iota \sqrt{k_y^2 + k_z^2} t)$, where const is a constant. While the integration is carried out over the entire k_y-k_z plane, there is a cutoff for the integration in the k_x coordinate for $\hat{k}_x \sim k$. Due to this, the integral for the autocorrelation function over wave number space is of the form $\int k^{D+1} dk \exp(\pm \text{const} \times \iota k t)$, which decreases proportional to $t^{-(D+1)}$, where D is the dimensionality of the system. Therefore, for the autocorrelation functions along the flow and gradient directions, we obtain

$$\langle u_x(\mathbf{x}(t),t)u_x(\mathbf{x}(0),0)\rangle \sim \langle u_y(\mathbf{x}(t),t)u_y(\mathbf{x}(0),0)\rangle \sim (\dot{\gamma} t)^{-(D+1)}. \quad (70)$$

This decrease is proportional to t^{-3} in two dimensions which is identical to Eqs. (67) and (68), and is proportional to t^{-4} in three dimensions, which is slightly slower than that in Eqs. (67) and (68). The autocorrelation function in the z direction in Eq. (69) decays proportional to $\exp(-\bar{\mu}^{\dagger} k^2 t)$. The cutoff in the wave number space for this mode is $\hat{k}_x \sim k^4$. Therefore, when the autocorrelation function for this mode is integrated over wave number space, we obtain an integral of the form $\int_{\mathbf{k}} k^{D+3} dk \exp(-\bar{\mu}^{\dagger} k^2 t)$, which is proportional to $t^{-(D+4)/2}$. Therefore, the equivalent of Eq. (68) for this case is

$$\langle u_z(\mathbf{x}(t),t)u_z(\mathbf{x}(0),0)\rangle \sim (\dot{\gamma} t)^{-(D+4)/2}. \quad (71)$$

In two dimensions, this contribution to the autocorrelation function decays as t^{-3}, which is identical to Eqs. (67) and (68), while in three dimensions, the decay is proportional to $t^{-7/2}$, which is slightly slower than that in Eq. (68).

III. CONCLUSIONS

The growth rates and eigenvectors for the linear hydrodynamic modes of a sheared inelastic fluid were calculated in Sec. III. It was found that the solutions for the growth rate depend on the relative magnitudes of the wavelength of the fluctuations and the "conduction length" $\lambda/(1-e)^{1/2}$, where λ is the mean free path and e is the coefficient of restitution. If the wavelength is small compared to the conduction length, then the rate of conduction of energy is large compared to the rate of dissipation, and it is appropriate to treat energy as a conserved variable. In this case, we recover the solutions of Lutsko and Dufty [10] for the growth rates of the hydrodynamic modes. The eigenvectors of the collision operator are also identical to Lutsko and Dufty [10] in the leading approximation in the small-k limit and are found to be form an orthonormal basis set. However, for the higher corrections, the eigenvectors are obtained by solving a differential equation in time; this is because the wave vector in the linear hydrodynamic matrix is time dependent. The procedure for obtaining the higher corrections was formulated, and the first correction for the eigenvector was also explicitly calculated.

In the limit where the wavelength of fluctuations is large compared to the conduction length, the rate of conduction in the energy balance equation is small compared to the rates of production and dissipation. In this case, energy is a nonconserved variable and the only conserved variables are the mass and the three components of the momentum. The scaling of the growth rates with wave number turns out to be very different in this case. As was shown earlier [14], there are three coupled modes for fluctuations in density and momentum in the plane of the shear. The growth rates of these modes are proportional to $k^{2/3}$ in the limit $k \to 0$. Either one or two of these modes are unstable in the short-time limit; however, these modes are stabilized at long times due to the turning of the wave vector. The fourth mode is a transverse diffusion mode, with decay rate proportional to k^2 in the limit $k \to 0$. The eigenvectors for these modes were also evaluated; in contrast to the eigenvectors for an elastic fluid, the leading-order eigenvectors in this case are not orthonormal. In an elastic fluid, the k^2 dependence of the decay rates of the hydrodynamic modes results in the long-time tails in the velocity autocorrelation functions, which decay proportional to t^{-1} and $t^{-3/2}$ in two and three dimensions, respectively. In an inelastic fluid, in contrast, the $k^{-4/5}$ dependence of the growth rates implies that the velocity autocorrelation function for the velocity in the flow and gradient directions decays proportional to $t^{-5/2}$ in two dimensions and proportional to $t^{-15/4}$ in three dimensions. The only exception is for perturbations with $k_x = 0$ (along the gradient-vorticity plane) for which the decay rates are proportional to $t^{-(D+1)}$. The autocorrelation function for the velocity in the vorticity direction shows a decay proportional to t^{-3} in two dimensions and $t^{-7/2}$ in three dimensions.

An earlier study [31] predicted a scaling of $t^{-3D/2}$ for the long-time tails of the velocity autocorrelation function. This was erroneous because of the assumption that the crossover from the short-time growth to the long-time decay would occur at $k^{2/3} \sim k^2 t^2$ for the growth rates in Eqs. (44). However, Eq. (45) shows that the growth rate in the short-time limit is actually $k^{2/3} t^{1/3}$, due to the dependence of k_y on time. Due to this, the crossover occurs at $k^{2/3} t^{1/3} \sim k^2 t^2$, resulting in a long-time decay proportional to $t^{-5D/4}$. This has been verified from the scaling of the wave-number-dependent integral time in Fig. 2. In experiments or simulations, the distinction between these two scalings would be difficult to distinguish because it would be necessary to track the decay of the autocorrelation function over three to four orders of magnitude, which would require an unrealistically large number of samples for statistical averaging.

While the calculations have provided us with expressions for the eigenvalues and eigenvectors, the calculation has involved an expansion in the parameter ϵ. In addition, it is necessary to calculate the eigenvectors iteratively, since the dispersion matrix is dependent on time. Due to these disadvantages, the procedure adopted here is not suitable for obtaining quantitative results, and more work has to be done to obtain better formulations. Another disadvantage is that the solutions for the eigenvalues and eigenvectors are not uniformly valid throughout the domain. The expressions for the growth rates obtained for $k_x/k \sim 1$ diverge in the limit $k_x/k \to 0$, and it is necessary to carry out a different asymptotic analysis in the latter regime. Another issue that needs further investigation is the dynamics of perturbations with $k_x=0$. The solutions obtained here, as well as earlier solutions [14], indicate that perturbations in the vorticity direction are unstable in the long-time limit while the integral over the wave vector space for these unstable modes was found to yield a finite result for the autocorrelation function based on scaling arguments. This result needs to be examined by further calculations where uniform approximations for the dispersion relations valid throughout the wave number domain are used. Matched asymptotic expansions may be one way to proceed.

The present results are used to determine the effect of correlations on the dynamics of a dilute sheared inelastic fluid in Part II.

ACKNOWLEDGMENT

This research was supported by the Department of Science and Technology, Government of India.

APPENDIX: EIGENVECTORS OF THE HYDRODYNAMIC MATRIX

Here, we discuss the solution of the matrix differential equation (35) for a system where the eigenvalue matrix $\mathbf{L}$ is a function of time due to the time dependence of the wave vector. In this case, the eigenvalue matrix $\mathbf{\Lambda}$ is also dependent on time.

It is difficult to solve Eq. (35), in general, to obtain the matrix $\mathbf{E}$. Progress can be made by realizing $(\partial/\partial t) \equiv \epsilon \dot{\gamma} k_x (\partial/\partial k_y)$, since the dependence of $\mathbf{E}$ on time is only through the dependence of k_y on time in Eq. (25). Therefore, we can use an expansion of $\mathbf{E}=\mathbf{E}^{(0)}+\mathbf{E}^{(1)}+\cdots$ and expand Eq. (35) to write

$$\mathbf{L}\mathbf{E}^{(0)} = \mathbf{E}^{(0)}\mathbf{\Lambda},$$

$$\mathbf{L}\mathbf{E}^{(i)} = \mathbf{E}^{(i)}\mathbf{\Lambda} - \frac{\partial \mathbf{E}^{(i-1)}}{\partial t}, \tag{A1}$$

for all $i \geq 1$. While the above expansion appears uncontrolled, it should be noted that $(\partial/\partial t) \equiv \epsilon \dot{\gamma} k_x (\partial/\partial k_y)$, and so the above expansion is a asymptotic in the parameter ϵ, though not in wave number. However, we prefer not to expand $\mathbf{L}$ and Γ in ϵ, as one would do in an asymptotic expansion, since Eqs. (A1) can be solved using the complete forms of $\mathbf{L}$ and Γ.

Equations (A1) are inhomogeneous equations which have to be solved for $\mathbf{E}^{(i)}$ at each order i. In order to solve these, it is first necessary to establish that the equations satisfy the solvability criteria. We first consider the solution for the first correction $(i=1)$ in Eqs. (A1):

$$\mathbf{L}\mathbf{E}^{(1)} = \mathbf{E}^{(1)}\mathbf{\Lambda} - \partial_t \mathbf{E}^{(0)}. \tag{A2}$$

If we rewrite the first correction to the generalized eigenvector as

$$\mathbf{E}^{(i)} = \mathbf{E}^{(0)}\mathbf{E}_*^{(i)}, \tag{A3}$$

we obtain

$$\mathbf{E}_*^{(i)}\mathbf{\Lambda} - \mathbf{\Lambda}\mathbf{E}_*^{(i)} = [(\mathbf{E}^{(0)})^{-1}\partial_t \mathbf{E}^{(0)}]\mathbf{E}_*^{(i-1)} + \partial_t \mathbf{E}_*^{(i-1)}. \tag{A4}$$

The above equation is an inhomogeneous equation, which has to be solved for $\mathbf{E}_*^{(i)}$. The following points should be noted about solving the equation.

(i) The left-hand side of Eq. (A4) is symmetric if $\mathbf{E}_*^{(1)}$ is antisymmetric and it is antisymmetric if $\mathbf{E}_*^{(1)}$ is symmetric. Therefore, the symmetric part of the solution for $\mathbf{E}_*^{(1)}$ depends on the antisymmetric part of the inhomogeneous term $[(\mathbf{E}^{(0)})^{-1}\partial_t \mathbf{E}^{(0)}]\mathbf{E}_*^{(i-1)} + \partial_t \mathbf{E}_*^{(i-1)}$ and vice versa.

(ii) In either case, it can easily be verified that the diagonal elements of the left-hand side of Eq. (A4) are zero. Therefore, a solution exists only if the diagonal elements of the inhomogeneous term on the right-hand side are zero. In the calculation for an elastic fluid, the eigenvectors are orthogonal, so $(\mathbf{E}^{(0)})^{-1}=(\mathbf{E}^{(0)})^{\dagger}$, where the superscript $\dagger$ is used for the transpose. In this case, it can easily be verified that $(\mathbf{E}^{(0)})^{\dagger}\partial_t \mathbf{E}^{(0)}$ is an antisymmetric matrix, and so the solvability condition is satisfied. In the calculation for an inelastic fluid, we verify that $(\mathbf{E}^{(0)})^{-1}\partial_t \mathbf{E}^{(0)}$ is an antisymmetric matrix, so that Eq. (A4) is solvable.

(iii) It should also be noted that the matrix elements on the left-hand side do not depend on the diagonal elements of $\mathbf{E}_*^{(i)}$. Therefore, these diagonal elements cannot be evaluated by solving Eq. (A4). However, they can be evaluated from the solvability condition for the second correction to the eigenvectors, $\mathbf{E}^{(i+1)}$, as follows.

The equation for the second correction to the eigenvectors $\mathbf{E}^{(i+1)}$ is

$$\mathbf{E}_*^{(i+1)}\mathbf{\Lambda} - \mathbf{\Lambda}\mathbf{E}_*^{(i+1)} = [(\mathbf{E}^{(0)})^{-1}\partial_t \mathbf{E}^{(0)}]\mathbf{E}_*^{(i)} + \partial_t \mathbf{E}_*^{(i)}. \tag{A5}$$

As in the case of the equation for $\mathbf{E}_*^{(i)}$ [Eq. (A4)], the diagonal elements of the matrix on the left-hand side of the above equation are identically zero. Therefore, the above equation is solvable only if all the diagonal elements of the matrix on the right-hand side are equal to zero:

$$\mathrm{diag}\{[(\mathbf{E}^{(0)})^{-1}\partial_t \mathbf{E}^{(0)}]\mathbf{E}_*^{(i)} + \partial_t \mathbf{E}_*^{(i)}\} = 0. \tag{A6}$$

Since the diagonal elements of $(\mathbf{E}^{(0)})^{-1}\partial_t \mathbf{E}^{(0)}$ are zero, the diagonal elements of the first term on the left do not depend on the diagonal elements of $\mathbf{E}_*^{(i)}$. Therefore, we obtain a set of first-order differential equation to be satisfied by the diag-

onal elements of $\mathbf{E}_*^{(i)}$. These are solved in order to obtain the diagonal components of the matrix $\mathbf{E}_*^{(i)}$.

The eigenvectors of Eq. (A1) $\mathbf{E}^{(0)}$ can be calculated to leading order in k. If we substitute $\lambda_1=\imath kc_s$, $\lambda_2=-\imath kc_s$, $\lambda_3=\lambda_4=\lambda_5=0$, and retain terms only to leading order in k, the matrix $\mathbf{L}$ can be reduced to a real symmetric matrix by dividing throughout by $\imath$. For this real symmetric matrix, the eigenvectors are orthonormal:

$$\mathbf{E}^{(0)}=\left[\begin{pmatrix}(\sqrt{2}c_s)^{-1}\\(k_x/\sqrt{2}k)\\(k_y/\sqrt{2}k)\\(k_z/\sqrt{2}k)\\(1/\sqrt{C_v})\end{pmatrix}\begin{pmatrix}(\sqrt{2}c_s)^{-1}\\(-k_x/\sqrt{2}k)\\(-k_y/\sqrt{2}k)\\(-k_z/\sqrt{2}k)\\(1/\sqrt{C_v})\end{pmatrix}\begin{pmatrix}0\\(k_xk_y/k\sqrt{k_x^2+k_z^2})\\-(k_xk_z/\sqrt{k_x^2+k_z^2})\\(k_yk_z/k\sqrt{k_x^2+k_z^2})\\0\end{pmatrix}\begin{pmatrix}0\\-(k_z/\sqrt{k_x^2+k_z^2})\\0\\(k_x/\sqrt{k_x^2+k_z^2})\\0\end{pmatrix}\begin{pmatrix}(c_s\sqrt{C_v})^{-1}\\0\\0\\0\\-c_s^{-1}\end{pmatrix}\right]. \tag{A7}$$

However, it should be noted that the $O(k)$ contribution to $\mathbf{L}$ is not Hermetian, and so the orthonormality of the eignevectors is valid only in the leading approximation in the small k limit.

The matrix $\mathbf{E}_*^{(1)}$ in the solution (A3) for the first correction $\mathbf{E}^{(1)}$ can be calculated using Eq. (A5) and (A6). The matrix $\mathbf{E}_*^{(1)}$ is symmetric because the inhomogeneous term in the right-hand side of Eq. (A5) is symmetric. The solution is of the form

$$\mathbf{E}_*^{(1)}=\left[\begin{pmatrix}e_{11}\\0\\e_{13}\\0\\0\end{pmatrix}\begin{pmatrix}0\\e_{22}\\e_{23}\\0\\0\end{pmatrix}\begin{pmatrix}e_{13}\\e_{23}\\0\\0\\0\end{pmatrix}\begin{pmatrix}0\\0\\0\\0\\0\end{pmatrix}\begin{pmatrix}0\\0\\0\\0\\0\end{pmatrix}\right], \tag{A8}$$

where

$$e_{11}=-e_{22}=-\frac{\imath\epsilon^2\dot{\gamma}^2}{2c_s}\int_{-\infty}^{t}dt'\frac{k_x^2(k_x^2+k_z^2)}{k^5},$$

$$e_{13}=e_{23}=\frac{\imath\epsilon\dot{\gamma}}{\sqrt{2}c_s}\frac{k_x\sqrt{k_x^2+k_z^2}}{k^3}. \tag{A9}$$

It should be noted that both the diagonal and off-diagonal terms in Eqs. (A9) are of equal magnitude. This is because when we integrate with respect to time for the diagonal terms, the only time-dependent term in the integrand is the component k_y through Eq. (25). This integration results in a factor $1/\epsilon\dot{\gamma}$ in the solutions for e_{11} and e_{22}, and the resultant expressions are linear in $\epsilon\dot{\gamma}$. Hence e_{11} and e_{22} are of the same magnitude as e_{13} and e_{23} in Eqs. (A9).

The eigenvectors can be obtained in a similar manner for the case $k\ll\epsilon$, for which the eigenvalues are given in Eqs. (44). Since the hydrodynamic matrix $\mathbf{L}$ is not symmetric for $k\ll\epsilon$, it is not possible to obtain an orthonormal set of eigenvectors. In the leading approximation, the basis vectors $\mathbf{E}^{(0)}$ can be determined by solving the equation $\mathbf{L}\mathbf{E}^{(0)}=\mathbf{E}^{(0)}\Lambda$, and the solutions for the basis vectors correct to leading order in a small-k expansion are obtained. The matrix $\mathbf{E}^{(0)}$, whose columns are the eigenevectors corresponding to the eigenvalues λ_1 to λ_4, is

$$\mathbf{E}^{(0)}=\left[\begin{pmatrix}(k^{2/3}s_0/\epsilon\dot{\gamma})\\1\\-(\imath k^{1/3}/s_0)\\(k_xk_z/k^{4/3}s_0^2)\end{pmatrix}\begin{pmatrix}-[(-1)^{2/3}k^{2/3}s_0/\epsilon\dot{\gamma}]\\1\\-[\imath k^{1/3}/(-1)^{2/3}s_0]\\(k_xk_z/[(-1)^{2/3}k^{2/3}s_0)^2]\end{pmatrix}\begin{pmatrix}-[(-1)^{4/3}k^{2/3}s_0/\epsilon\dot{\gamma}]\\1\\-[\imath k^{1/3}/(-1)^{4/3}s_0]\\\{k_xk_z/[(-1)^{4/3}k^{2/3}s_0]^2\}\end{pmatrix}\begin{pmatrix}0\\-(k_z/\sqrt{k_x^2+k_z^2})\\0\\(k_x/\sqrt{k_x^2+k_z^2})\end{pmatrix}\right]. \tag{A10}$$

Since the eigenvectors are not orthonormal, the duals of the eigenvectors are the rows of the matrix $(\mathbf{E}^{(0)})^{-1}$. As intuitively expected, the transverse eigenvector corresponding to the growth rate λ_4 in Eqs. (44), which is the fourth column of $\mathbf{E}^{(0)}$, is identical to that for an elastic system, Eq. (A7).

The matrix $\mathbf{E}_*^{(1)}$ in the solution (A3) for the first correction $\mathbf{E}^{(1)}$ can be calculated using Eqs. (A5) and (A6). The matrix $\mathbf{E}_*^{(1)}$ is symmetric because the inhomogeneous term in the right-hand side of Eq. (A5) is symmetric. The solution is of the form

$$\mathbf{E}_*^{(1)}=\left[\begin{pmatrix}e_{11}\\e_{12}\\e_{13}\\0\end{pmatrix}\begin{pmatrix}e_{12}\\e_{22}\\e_{23}\\0\end{pmatrix}\begin{pmatrix}e_{13}\\e_{23}\\e_{33}\\0\end{pmatrix}\begin{pmatrix}0\\0\\0\\0\end{pmatrix}\right], \tag{A11}$$

where

$$e_{11}=(-1)^{2/3}e_{22}=(-1)^{4/3}e_{33}=-\frac{\epsilon^2\dot{\gamma}^2}{3}\int_{-\infty}^{t}dt'\frac{k_x^2}{s_0^3}\left(\frac{ds_0}{dk_y}\right)^2,$$

$$e_{23}=(-1)^{(2/3)}e_{13}=(-1)^{(4/3)}e_{12}=\frac{\epsilon\dot{\gamma}}{3s_0^2}\left(k_x\frac{\partial s_0}{\partial k_y}\right). \tag{A12}$$

Finally, we note that though Eq. (35) could also be solved by expanding out the hydrodynamic matrix $\mathbf{L}$ in a series in the ϵ, it is more difficult to obtain the completeness and solvability conditions in this case. Consider an expansion of the hydrodynamic matrix as

$$\mathbf{L}=\mathbf{L}^{(0)}+\mathbf{L}^{(1)}+\mathbf{L}^{(2)}+\cdots. \tag{A13}$$

Using the same procedure as that used in at the beginning of the Appendix, the equivalent of Eqs. (A1) is

$$\mathbf{L}^{(0)}\mathbf{E}^{(0)}=\mathbf{E}^{(0)}\mathbf{\Lambda},$$

$$\mathbf{L}^{(0)}\mathbf{E}^{(i)} = \mathbf{E}^{(i)}\mathbf{\Lambda} - \frac{\partial \mathbf{E}^{(i-1)}}{\partial t} - \sum_{j=1}^{i} \mathbf{L}^{(j)}\mathbf{E}^{(i-j)}, \tag{A14}$$

where the last term on the right-hand side of Eq. (A14) accounts for the expansion of the matrix $\mathbf{L}$. If Eq. (A3) is used for $\mathbf{E}^{(i)}$, then Eq. (A14) becomes

$$\mathbf{E}_*^{(i)}\mathbf{\Lambda} - \mathbf{\Lambda}\mathbf{E}_*^{(i)} = [(\mathbf{E}^{(0)})^{-1}\partial_t \mathbf{E}^{(0)}] + \partial_t \mathbf{E}_*^{(i-1)} - \sum_{j=1}^{i} \mathbf{L}^{(j)}\mathbf{E}^{(0)}\mathbf{E}_*^{(i-j)}. \tag{A15}$$

The above equation is identical in form to Eq. (A4), except that it has additional inhomogeneous terms on the right-hand side. The left-hand side of Eq. (A15) does not depend on the diagonal elements of the matrix $\mathbf{E}_*^{(i)}$, and so the off-diagonal terms in the matrix can be obtained by solving Eq. (A15). The diagonal elements of the matrix $\mathbf{E}_*^{(i-1)}$ are obtained by the condition that the diagonal elements of the right-hand side of Eq. (A15) are zero:

$$\mathrm{diag}([(\mathbf{E}^{(0)})^{-1}\partial_t \mathbf{E}^{(0)}]\mathbf{E}_*^{(i)} + \partial_t \mathbf{E}_*^{(i)} - \sum_{j=1}^{i} \mathbf{L}^{(j)}\mathbf{E}^{(0)}\mathbf{E}_*^{(i-j)}) = 0. \tag{A16}$$

Equation (A16) is more difficult to solve than Eq. (A6), since the latter contains the additional inhomogeneous terms on the left, whereas Eq. (A6) depends only on $\mathbf{E}_*^{(i)}$ and $\mathbf{E}^{(0)}$. Therefore, Eq. (A6) can be solved from just the off-diagonal terms of $\mathbf{E}_*^{(i)}$ and the leading-order eigenvector $\mathbf{E}^{(0)}$, whereas it is necessary to include additional inhomogeneous terms on the right-hand side to solve Eq. (A16). In addition, the solutions of Eqs. (A4) and (A6) contain the complete $\mathbf{L}$ matrix, and so the solutions at order i contain additional terms which are higher order in the ϵ expansion, even though the are accurate only up to ϵ^i.

[1] D. Ronis, Physica A **99**, 403 (1979).
[2] S. B. Savage and D. J. Jeffrey, J. Fluid Mech. **110**, 255 (1981).
[3] J. T. Jenkins and S. B. Savage, J. Fluid Mech. **130**, 187 (1983).
[4] J. T. Jenkins and M. W. Richman, J. Fluid Mech. **171**, 53 (1986).
[5] C. K. K. Lun, J. Fluid Mech. **233**, 539 (1991).
[6] N. Sela and I. Goldhirsch, J. Fluid Mech. **361**, 41 (1998).
[7] J. J. Brey, J. W. Dufty, C.-S. Kim, and A. Santos, Phys. Rev. E **58**, 4638 (1998).
[8] V. Kumaran, Phys. Rev. E **57**, 5660 (1998).
[9] M. Ernst, B. Cichoki, J. Dorfman, J. Sharma, and H. van Beijeren, J. Stat. Phys. **18**, 237 (1978).
[10] J. Lutsko and J. W. Dufty, Phys. Rev. A **32**, 1229 (1985).
[11] S. B. Savage, J. Fluid Mech. **241**, 109 (1992).
[12] M. Babic, J. Fluid Mech. **254**, 127 (1993).
[13] M. Alam and P. R. Nott, J. Fluid Mech. **343**, 267 (1997).
[14] V. Kumaran, J. Fluid Mech. **506**, 1 (2004).
[15] M. Lee and J. W. Dufty, Phys. Rev. E **56**, 1733 (1997).
[16] M. Alam and P. R. Nott, J. Fluid Mech. **377**, 99 (1998).
[17] K. Saitoh and H. Hayakawa, Phys. Rev. E **75**, 021302 (2007).
[18] K. Kawasaki and J. Gunton, Phys. Rev. A **8**, 2048 (1973).
[19] T. Yamada and K. Kawasaki, Prog. Theor. Phys. **53**, 111 (1975).
[20] M. Ernst and J. Dorfman, Physica (Amsterdam) **61**, 157 (1972).
[21] B. Alder and T. Wainwright, Phys. Rev. A **1**, 18 (1970).
[22] I. Goldhirsch and T. P. C. van Noije, Phys. Rev. E **61**, 3241 (2000).
[23] J. Dufty, A. Baskaran, and J. J. Brey, Phys. Rev. E **77**, 031310 (2008).
[24] A. Baskaran, J. W. Dufty, and J. J. Brey, Phys. Rev. E **77**, 031311 (2008).
[25] T. P. C. van Noije and M. H. Ernst, e-print arXiv:cond-mat/9803042; J. S. van Zon and F. C. MacKintosh, Phys. Rev. Lett. **93**, 038001 (2004).
[26] I. Goldhirsch and G. Zanetti, Phys. Rev. Lett. **70**, 1619 (1993); T. P. C. van Noije, M. H. Ernst, and R. Brito, Phys. Rev. E **57**, R4891 (1998).
[27] V. Kumaran, Phys. Fluids **13**, 2258 (2001).
[28] V. Kumaran, Physica A **293**, 385 (2001).
[29] V. Kumaran, J. Fluid Mech. **561**, 1 (2006).
[30] V. Kumaran, Europhys. Lett. **73**, 232 (2006).
[31] V. Kumaran, Phys. Rev. Lett. **96**, 258002 (2006).
[32] V. Kumaran, J. Fluid Mech. **599**, 121 (2008).
[33] M. Otsuki and H. Hayakawa, e-print arXiv:cond-mat/0711.1421.
[34] S. Chapman and T. G. Cowling, *The Mathematical Theory of Non-uniform Gases* (Cambridge University Press, Cambridge, U.K., 1970).